[6] T. Browder, C.E. Butterfield, B.M. Kraling, B. Shi, B. Marshall, M.S. O'Reilly, J. Folkman, Antiangiogenic scheduling of chemotherapy improves efficacy against experimental drug-resistant cancer, Cancer Res. 60 (2000) 1878–1886.
[7] H. Maeda, J. Wu, T. Sawa, Y. Matsumura, K. Hori, Tumor vascular permeability and the EPR effect in macromolecular therapeutics: a review, J. Control. Release 65 (2000) 271–284.
[8] R.K. Jain, Delivery of molecular and cellular medicine to solid tumors, Adv. Drug Deliv. Rev. 46 (2001) 149–168.
[9] D. Papahadjopoulos, T.M. Allen, A. Gabizon, E. Mayhew, K. Matthay, S.K. Huang, K.D. Lee, M.C. Woodle, D.D. Lasic, C. Redemann, F.J. Martin, Sterically stabilized liposomes: improvements in pharmacokinetics and antitumor therapeutic efficacy, Proc. Natl. Acad. Sci. U. S. A. 88 (1991) 11460–11464.
[10] A. Gabizon, R. Catane, B. Uziely, B. Kaufman, T. Safra, R. Cohen, F. Martin, A. Huang, Y. Barenholz, Prolonged circulation time and enhanced accumulation in malignant exudates of doxorubicin encapsulated in polyethylene-glycol coated liposomes, Cancer Res. 54 (1994) 987–992.
[11] J. Vaage, D. Donovan, E. Mayhew, R. Abra, A. Huang, Therapy of human ovarian carcinoma xenografts using doxorubicin encapsulated in sterically stabilized liposomes, Cancer 72 (1993) 3671–3675.
[12] S.E. Krown, D.W. Northfelt, D. Osoba, J.S. Stewart, Use of liposomal anthracyclines in Kaposi's sarcoma, Semin. Oncol. 31 (2004) 36–52.
[13] T. Safra, F. Muggia, S. Jeffers, D.D. Tsao-Wei, S. Groshen, O. Lyass, R. Henderson, G. Berry, A. Gabizon, Pegylated liposomal doxorubicin (doxil): reduced clinical cardiotoxicity in patients reaching or exceeding cumulative doses of 500 mg/m^2, Ann. Oncol. 11 (2000) 1029–1033.
[14] T. Ishida, R. Maeda, M. Ichihara, K. Irimura, H. Kiwada, Accelerated clearance of PEGylated liposomes in rats after repeated injections, J. Control. Release 88 (2003) 35–42.
[15] E. Shiraga, J.M. Barichello, T. Ishida, H. Kiwada, A metronomic schedule of cyclophosphamide combined with PEGylated liposomal doxorubicin has a highly antitumor effect in an experimental pulmonary metastatic mouse model, Int. J. Pharm. 353 (2008) 65–73.
[16] G.R. Bartlett, Colorimetric assay methods for free and phosphorylated glyceric acids, J. Biol. Chem. 234 (1959) 469–471.
[17] E.M. Bolotin, R. Cohen, L.K. Bar, S.N. Emanuel, D.D. Lasic, Y. Barenholz, Ammonium sulphate gradients for efficient and stable remote loading of amphipathic weak bases into liposomes and ligandosomes, J. Liposome. Res. 4 (1994) 455–479.
[18] D. Fukumura, Role of microenvironment on gene expression, angiogenesis and microvascular functions in tumors, in: G.G. Meadows (Ed.), Integration/Interaction of Oncologic Growth, Springer Science+Business Media B.V, Dordrecht, 2005, pp. 23–36.
[19] R.K. Jain, Normalization of tumor vasculature: an emerging concept in antiangiogenic therapy, Science 307 (2005) 58–62.
[20] F. Winkler, S.V. Kozin, R.T. Tong, S.S. Chae, M.F. Booth, I. Garkavtsev, L. Xu, D.J. Hicklin, D. Fukumura, E. di Tomaso, L.L. Munn, R.K. Jain, Kinetics of vascular normalization by VEGFR2 blockade governs brain tumor response to radiation: role of oxygenation, angiopoietin-1, and matrix metalloproteinases, Cancer Cell. 6 (2004) 553–563.
[21] D. Fukumura, R.K. Jain, Tumor microvasculature and microenvironment: targets for anti-angiogenesis and normalization, Microvasc. Res. 74 (2007) 72–84.
[22] R.K. Jain, R.T. Tong, L.L. Munn, Effect of vascular normalization by antiangiogenic therapy on interstitial hypertension, peritumor edema, and lymphatic metastasis: insights from a mathematical model, Cancer Res. 67 (2007) 2729–2735.
[23] Y. Hamano, H. Sugimoto, M.A. Soubasakos, M. Kieran, B.R. Olsen, J. Lawler, A. Sudhakar, R. Kalluri, Thrombospondin-1 associated with tumor microenvironment contributes to low-dose cyclophosphamide-mediated endothelial cell apoptosis and tumor growth suppression, Cancer Res. 64 (2004) 1570–1574.
[24] J. Lawler, Thrombospondin-1 as an endogenous inhibitor of angiogenesis and tumor growth, J. Cell. Mol. Med. 6 (2002) 1–12.
[25] R.T. Tong, Y. Boucher, S.V. Kozin, F. Winkler, D.J. Hicklin, R.K. Jain, Vascular normalization by vascular endothelial growth factor receptor 2 blockade induces a pressure gradient across the vasculature and improves drug penetration in tumors, Cancer Res. 64 (2004) 3731–3736.
[26] M.R. Kano, Y. Bae, C. Iwata, Y. Morishita, M. Yashiro, M. Oka, T. Fujii, A. Komuro, K. Kiyono, M. Kaminishi, K. Hirakawa, Y. Ouchi, N. Nishiyama, K. Kataoka, K. Miyazono, Improvement of cancer-targeting therapy, using nanocarriers for intractable solid tumors by inhibition of TGF-beta signaling, Proc. Natl. Acad. Sci. U. S. A. 104 (2007) 3460–3465.
[27] T.L. Ten Hagen, A.H. Van Der Veen, P.T. Nooijen, S.T. Van Tiel, A.L. Seynhaeve, A.M. Eggermont, Low-dose tumor necrosis factor-alpha augments antitumor activity of stealth liposomal doxorubicin (DOXIL) in soft tissue sarcoma-bearing rats, Int. J. Cancer 87 (2000) 829–837.
[28] A.L. Seynhaeve, S. Hoving, D. Schipper, C.E. Vermeulen, G. de Wiel-Ambagtsheer, S.T. van Tiel, A.M. Eggermont, T.L. Ten Hagen, Tumor necrosis factor alpha mediates homogeneous distribution of liposomes in murine melanoma that contributes to a better tumor response, Cancer Res. 67 (2007) 9455–9462.
[29] P.K. Singal, N. Iliskovic, Doxorubicin-induced cardiomyopathy, N. Engl. J. Med. 339 (1998) 900–905.
[30] B. Uziely, S. Jeffers, R. Isacson, K. Kutsch, D. Wei-Tsao, Z. Yehoshua, E. Libson, F.M. Muggia, A. Gabizon, Liposomal doxorubicin: antitumor activity and unique toxicities during two complementary phase I studies, J. Clin. Oncol. 13 (1995) 1777–1785.
[31] F.D. Goebel, D. Goldstein, M. Goos, H. Jablonowski, J.S. Stewart, Efficacy and safety of Stealth liposomal doxorubicin in AIDS-related Kaposi's sarcoma. The International SL-DOX Study Group, Br. J. Cancer 73 (1996) 989–994.
[32] D.W. Northfelt, F.J. Martin, P. Working, P.A. Volberding, J. Russell, M. Newman, M.A. Amantea, L.D. Kaplan, Doxorubicin encapsulated in liposomes containing surface-bound polyethylene glycol: pharmacokinetics, tumor localization, and safety in patients with AIDS-related Kaposi's sarcoma, J. Clin. Pharmacol. 36 (1996) 55–63.
[33] M.I. Koukourakis, S. Koukouraki, A. Giatromanolaki, S.C. Archimandritis, J. Skarlatos, K. Beroukas, J.G. Bizakis, G. Retalis, N. Karkavitsas, E.S. Helidonis, Liposomal doxorubicin and conventionally fractionated radiotherapy in the treatment of locally advanced non-small-cell lung cancer and head and neck cancer, J. Clin. Oncol. 17 (1999) 3512–3521.
[34] A.J. Quesada, T. Nelius, R. Yap, T.A. Zaichuk, A. Alfranca, S. Filleur, O.V. Volpert, J.M. Redondo, In vivo upregulation of CD95 and CD95L causes synergistic inhibition of angiogenesis by TSP1 peptide and metronomic doxorubicin treatment, Cell. Death Differ. 12 (2005) 649–658.

Journal of Controlled Release 137 (2009) 8–14

Contents lists available at ScienceDirect

Journal of Controlled Release

journal homepage: www.elsevier.com/locate/jconrel

Oxaliplatin encapsulated in PEG-coated cationic liposomes induces significant tumor growth suppression via a dual-targeting approach in a murine solid tumor model

Amr S. Abu Lila, Shinji Kizuki, Yusuke Doi, Takuya Suzuki, Tatsuhiro Ishida *, Hiroshi Kiwada

Department of Pharmacokinetics and Biopharmaceutics, Subdivision of Biopharmaceutical Sciences, Institute of Health Biosciences, The University of Tokushima, 1-78-1, Sho-machi, Tokushima 770-8505, Japan

ARTICLE INFO

Article history:
Received 15 January 2009
Accepted 27 February 2009
Available online 12 March 2009

Keywords:
Anticancer therapy
Drug delivery system
Anticancer drug
Oxaliplatin
PEG-coated cationic liposomes

ABSTRACT

We recently designed a PEG-coated cationic liposome targeted to angiogenic vessels and showed, in a murine dorsal air sac model, potent anti-angiogenic activity of an oxaliplatin (l-OHP) formulation of this liposome. In the present study, we extended the l-OHP formulation to a murine tumor-xenograft model. Following three injections, l-OHP containing PEG-coated cationic liposomes showed substantial tumor growth suppression and increased survival time of tumor-bearing mice without apparent side effects, compared with other l-OHP containing PEG-coated neutral liposomes and free l-OHP. In vivo imaging showed a preferential tumor accumulation and a broader distribution of PEG-coated cationic liposomes, compared with PEG-coated neutral liposomes. In addition, PEG-coated cationic liposomes delivered larger amounts of l-OHP into the tumor tissue than other l-OHP formulations, correlating with its antitumor efficiency. In vitro studies indicated that PEG-coated cationic liposomes were internalized not only by tumor cells but also by endothelial cells, and consequently its l-OHP formulation displayed higher cytotoxicity towards both cell types as compared with l-OHP containing PEG-coated neutral liposomes. In summary, l-OHP containing PEG-coated cationic liposomes induced significant tumor growth suppression, presumably by delivering encapsulated l-OHP into both tumor endothelial cells and tumor cells. Such dual targeting approach, i.e. vascular-targeting and tumor-targeting with a single liposomal l-OHP formulation, may have great potential for overcoming some major limitations in conventional chemotherapy.

1. Introduction

Oxaliplatin (l-OHP), a cisplatin derivative, has been approved for standard first- and second-line treatment of metastatic or advanced-stage colorectal cancer in combination with the infusion of 5-fluorouracil (5-FU)/leucovorin (FOLFOX) [1–3]. However, when used alone, its clinical efficiency is limited by the dose-limiting side effects such as neurotoxicity [4–6] and by high partitioning to erythrocytes in vivo [6]. Substantial efforts have been dedicated to solve these problems. One of the most intriguing strategies to overcome these drawbacks is to encapsulate l-OHP in a targetable drug delivery system such as liposomes [7–9].

Recently, we designed a polyethylene glycol (PEG)-coated cationic liposome to target the newly formed angiogenic vessels and developed a l-OHP formulation based on these liposomes. This targeted liposomal l-OHP formulation showed a remarkable in vivo anti-angiogenic activity in a mouse dorsal air sac (DAS) model [10]. Cationic liposomes have been reported to display a strong binding ability to tumor-derived angiogenic vascular endothelial cells and tumor cells due to the strong electrostatic adhesion between the cationic surface and the plasma membrane of cells [11–13]. In addition, grafting of PEG to the surface of the liposome may extend the circulation lifetime of the cationic liposome by preventing interactions with the biological in vivo environment [14–16]. This results in extensive extravasation of the liposomes due to the tumor-selective enhanced permeability and retention (EPR) effect [17], ultimately leading to enhanced accumulation of the liposomes in the tumor interstitium. We hypothesized that the specific properties of our PEG-coated cationic liposomes might enhance their chance to gain access not only to the endothelial cells in the originally targeted angiogenic vessels but also to the tumor cells following extravasation into the interstitial space. Hence, we assumed that, by our dual targeting approach to both endothelial cells in angiogenic vessels and

Abbreviations: CHOL, cholesterol; DC-6-14, O,O′-ditetradecanoyl-N-(alpha trimethyl ammonioacetyl)diethanolamine chloride; DiI, 1,1′-dioctadecyl-3,3,3′,3′-tetramethylindocarbocyanine perchlorate; DMEM, Dulbecco's modified Eagle's medium; EDTA, ethylenediamine tetraacetic acid; EGF, epidermal growth factor; FBS, fetal bovine serum; FCS, fetal calf serum; 5FU, 5-flourouracil; GA, gentamicin sulfate; HSPC, hydrogenated soya phosphatidylcholine; HUVEC, Human umbilical vascular endothelial cells; IGF-1, insulin-like growth factor; LLCC, Lewis lung carcinoma cells; l-OHP, oxaliplatin; $mPEG_{2000}$-DSPE, 1,2-distearoyl-sn-glycero-3-phosphoethanolamine-*n*-[methoxy (polyethyleneglycol)-2000]; MTT, 3-(4,5-dimethylthiazol-2-yl)-2,5 diphenyl tetrazolium bromide; PBS, Phosphate buffered saline; Pt, platinum; VEGF, vascular endothelial growth factor.

* Corresponding author. Tel./fax: +81 88 633 7260.
E-mail address: ishida@ph.tokushima-u.ac.jp (T. Ishida).

0168-3659/$ – see front matter © 2009 Elsevier B.V. All rights reserved.
doi:10.1016/j.jconrel.2009.02.023

tumor cells [18,19], l-OHP containing PEG-coated cationic liposomes will show markedly enhanced antitumor activity, as compared to l-OHP containing PEG-coated neutral liposomes (conventional PEG-coated liposomes).

In this study, we therefore investigated the therapeutic activity of l-OHP containing PEG-coated cationic liposomes in an in vivo murine solid tumor model. In addition, we evaluated the potential of the liposomes to extend the delivery of adequate quantities of l-OHP to tumors in vivo and to kill both tumor cells (Lewis lung carcinoma cells (LLCC)) and human umbilical vascular endothelial cells (HUVEC) in vitro.

2. Materials and methods

2.1. Materials

Hydrogenated soy phosphatidylcholine (HSPC) and 1,2-distearoyl-sn-glycero-3-phosphoethanolamine-*n*-[methoxy (polyethyleneglycol)-2000] ($mPEG_{2000}$-DSPE) were generously donated by NOF (Tokyo, Japan). Oxaliplatin (l-OHP) was generously donated by Taiho Pharmaceutical (Tokyo, Japan). Cholesterol (CHOL) and O,O′-ditetradecanoyl-N-(alpha-trimethyl ammonio acetyl) diethanolamine chloride (DC-6-14) were purchased from Sogo Pharmaceutical (Tokyo, Japan). 1,1′-dioctadecyl-3,3,3′,3′-tetramethyl-indocarbocyanine perchlorate (DiI) was purchased from Invitrogen (OR, USA). 3-(4,5-dimethylthiazol-2-yl)-2,5-diphenyltetrazolium bromide (MTT) was purchased from Nacalai Tesque (Kyoto, Japan). All other reagents were of analytical grade.

2.2. Animals and tumor cell line

Male C57BL/6 mice, 4 weeks old, were purchased from Japan SLC (Shizuoka, Japan). The experimental animals were allowed free access to water and mouse chow, and were housed under controlled environmental conditions (constant temperature, humidity, and 12 h dark–light cycle). All animal experiments were evaluated and approved by the Animal and Ethics Review Committee of the University of Tokushima. Lewis lung carcinoma cell (LLCC) line was purchased from Cell Resource Center for Biomedical Research (Institute of Development, Aging and Cancer, Tohoku University). LLCC line was maintained in Dulbecco's modified Eagle's medium (DMEM) (Nissui Pharmaceutical Co. Ltd., Tokyo, Japan) supplemented with 10% heat-inactivated FBS (Japan Bioserum, Hiroshima, Japan), 10 mM L-glutamine, 100 U/ml penicillin and 100 μg/ml streptomycin in a 5% CO_2/air incubator at 37 °C. Human umbilical vascular endothelial cells (HUVEC) were maintained in EBM-2 medium (Cambrex Bioscience, Walkersville, MD, USA) containing 10% fetal calf serum (FCS), vascular endothelial growth factor (VEGF), insulin-like growth factor (IGF-1), ascorbic acid, epidermal growth factor (EGF), GA-100 and heparin.

2.3. Preparation of liposomes

Cationic liposomes modified with $mPEG_{2000}$-DSPE were composed of HSPC/CHOL/DC-6-14/$mPEG_{2000}$-DSPE (2/1/0.2/0.2 molar ratio). Neutral liposomes modified with $mPEG_{2000}$-DSPE were composed of HSPC/CHOL/$mPEG_{2000}$-DSPE (2/1/0.2 molar ratio). For cellular uptake experiments and in vivo imaging experiments, 1 mol% of the fluorescent dye DiI was incorporated in the lipid mixture. All liposomes were prepared according to the method described earlier [10]. Briefly, lipids (50 mmol) were dissolved in 6 ml of chloroform/diethyl ether (1:2 v/v) and then 2 ml of l-OHP solution (8 mg/ml) in 5% (w/v) dextrose was dropped into the lipid mixture to form a w/o emulsion. For preparation of empty PEG-coated cationic liposomes, 5% dextrose solution was added instead of l-OHP solution. The volume ratio of the aqueous to the organic phase was maintained at 1:3. The emulsion was sonicated for 15 min and then the organic phase was removed to form liposomes by evaporation in a rotary evaporator at 40 °C under reduced pressure at 250 hPa for 1 h. The resulting liposomes were extruded through a polycarbonate membrane (200 nm pore size) using an extruder device (Lipex Biomembranes Inc., Vancouver, Canada) maintained at 65 °C to obtain liposomes with approximately 200 nm in a mean diameter. The phospholipid concentration was determined by colorimetric assay [20]. Un-encapsulated, free l-OHP was removed by dialysis by means of a dialysis cassette (Slyde-A-Lyzer, 10000MWCO, PIERCE, IL, USA) against 5% dextrose. Encapsulated l-OHP was quantified using an atomic absorption photometer (Z-5700, Hitachi, Tokyo, Japan). The size and zeta potential of the liposomes were determined by using a NICOMP 370 HPL submicron particle analyzer (Particle Sizing System, CA, USA). The encapsulation efficiency of l-OHP was calculated by dividing the drug to lipid ratio after the dialysis by the initial drug to lipid ratio. The encapsulation efficiency was approximately 20% in both liposomes. These values are three times higher than that reported recently by other group [7]. The physicochemical properties and encapsulation efficiency of the liposome preparations are summarized in Table 1.

2.4. Cellular uptake experiments

2.4.1. Cellular uptake of DiI-labeled liposomes

LLCC (2.5×10^4) were seeded onto 12-well plates in 1 ml of DMEM containing 10% FBS and pre-incubated for 24 h. HUVEC (2.5×10^4) were also seeded onto 12-well plates in 1 ml EBM-2 medium containing 10% serum for 24 h. After removal of culture medium, 1 ml of fresh medium containing either DiI-labeled PEG-coated neutral or cationic liposomes (4 μmol of lipids/well) was added, followed by incubation at 37 °C. At 4, 8, 12 and 24 h post-incubation, the cells were trypsinized following a single washing with cold phosphate buffered saline (PBS, 37 mM NaCl, 2.7 mM KCl, 8.1 mM Na_2HPO_4 and 1.47 mM KH_2PO_4; pH 7.4). The cells were collected into a 1.5 ml-Eppendorf tube and then treated for 5 min at room temperature with 0.3% trypan blue to quench extracellular fluorescence [21], followed by washing twice with PBS. This step is necessary in order to differentiate between membrane-bound and internalized liposomes. The cells were re-suspended in 200 μl of PBS containing 0.5 mM EDTA (EDTA-PBS). The cellular uptake of DiI-labeled liposomes was quantified using a flow cytometer with a Guava EastCyte™ MiniSystem (Guava Technologies, CA, USA) equipped with an argon-ion laser and 560 nm band pass filters for emission measurements. Approximately 10,000 events were acquired per sample, and the data were analyzed using Guava Express Plus software.

2.4.2. Uptake mechanism

To investigate the mechanism of internalization of DiI-labeled PEG-coated cationic liposome, LLCC (2.5×10^4) were seeded onto 24-well plates in 1 ml DMEM containing 10% FBS for 24 h.

HUVEC (2.5×10^4) were also seeded onto 24-well plates in 1 ml EBM-2 medium containing 10% FCS for 24 h. After pre-incubation, the culture medium was removed and the cells were further incubated for 30 min in the absence or presence of one of the following uptake inhibitors: sucrose (0.45 M) to inhibit formation of clathrin-coated vesicles, filipin (500 μg/ml) to inhibit caveolae-mediated uptake, or

Table 1
Physicochemical properties of liposomal l-OHP formulations.

Formulation	Particle size (nm)	Loading efficiency (%)	Zeta potential (mV)
PEG-coated cationic liposome	202.4 ± 14.7	23.6 ± 1.1	+11.5 ± 0.9
PEG-coated neutral liposome	200.4 ± 17.2	17.2 ± 3.7	−7.2 ± 0.5

Data were obtained with three liposome preparations which were prepared independently.

amiloride (10 mM) to inhibit macropinocytosis. Then, DiI-labeled PEG-coated cationic liposomes (4 μmol of lipid/well) were added and the cells were incubated for 1 h at 37 °C in the presence or absence of the inhibitor. The cells were washed once with 1 ml PBS and collected after trypsinisation followed by centrifugation (300 ×g, 4 °C, 5 min). To quench extracellular fluorescence (not internalized liposomes), the cells were treated with 0.3% trypan blue for 5 min at room temperature and resuspended in 0.2 ml of 0.5 mM EDTA-PBS. The cell suspension was analyzed by a flow cytometer as described above.

2.5. Cytotoxicity assay

Cytotoxicity of various l-OHP formulations was determined by MTT assay, as described previously [22]. Briefly, cells (LLCC or HUVEC) were seeded onto 96-well plates at a density of 5×10^2 cells per well 24 h prior to drug addition. The culture medium was replaced with fresh medium (DMEM for LLCC and EBM-2 for HUVEC) containing various concentrations of either free l-OHP, PEG-coated cationic liposomal l-OHP, PEG-coated neutral liposomal l-OHP, or empty PEG-coated cationic liposomes. Following 4 h incubation at 37 °C, the cells were washed twice with PBS and cultured in fresh medium for a further 48 h. After removing the media, 50 μl of MTT stock solution (5 mg/ml in PBS) was added to each well. The cells were further incubated at 37 °C for 4 h. Then, 150 μl of an acidic isopropanol solution (containing 0.04 N HCl) was added to each well to dissolve formazan crystals. The absorbance of each well was read at 570 nm on a microplate reader, Wallac 1420 ARVOsx (PerkinElmer, Trukn, Finland).

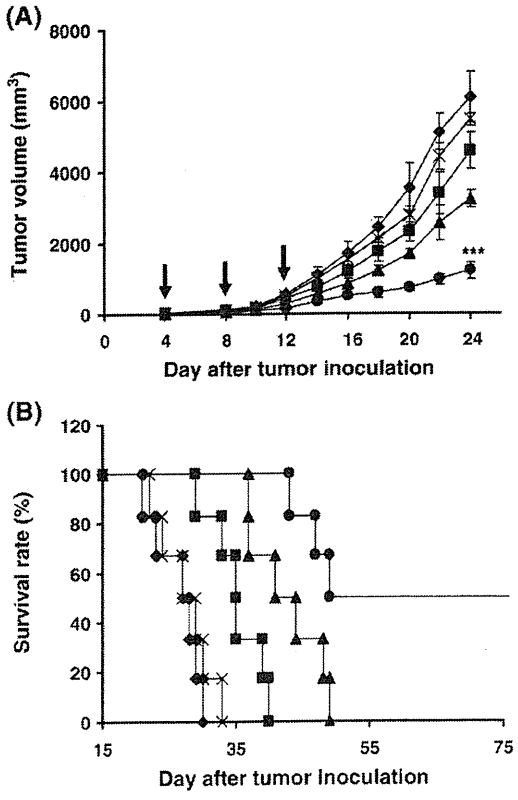

Fig. 1. Antitumor efficacy of various l-OHP formulations on LLCC-tumor bearing mice. On days 4, 8 and 12 after tumor inoculation (indicated by arrows), either free l-OHP (■), l-OHP containing PEG-coated cationic liposomes (●), l-OHP containing PEG-coated neutral liposomes (▲), empty PEG-coated cationic liposomes (x) or 5% dextrose solution (control) (♦) was administered via tail vein at a 1-OHP dose of 5 mg/kg. Each treatment group contained 6 mice. (A) Antitumor activity as assessed by tumor size and (B) survival of LLCC-bearing mice. Data in (A) represent mean ± S.D ($n=6$). ***$p<0.01$ against other formulations.

Table 2
Summary of median survival time (MST) and percent increased life span (ILS (%)) of tumor-bearing mice after treatment with various l-OHP formulations.

Formulation	MST (days) Median ± SD	ILS (%)
Control (5% dextrose solution)	27.5 ± 3.5	–
Empty PEG-coated cationic liposomes	28.0 ± 4.0	1.8%
Free l-OHP	35.0 ± 3.9	27.3%
PEG-coated neutral l-OHP liposomes	42.0 ± 5.2	52.7%
PEG-coated cationic l-OHP liposomes	> 70.0	> 150.0%

Data were obtained from Fig. 1B. MST and ILS(%) were calculated with the equations described in the Materials and methods section.

2.6. Evaluation of therapeutic efficacy of l-OHP formulations in the Lewis lung carcinoma bearing mouse model

Male C57BL/6 mice were inoculated subcutaneously (s.c.) at the flank region with LLCC (5×10^5) in a volume of 100 μl (PBS). The mice were divided into five groups. On days 4, 8 and 12 after tumor inoculation, each group (6 mice) received three intravenous injections of either 5% dextrose (control), free l-OHP (5 mg/kg), PEG-coated cationic l-OHP liposomes (5 mg l-OHP/kg), PEG-coated neutral l-OHP liposomes (5 mg l-OHP/kg) or empty PEG-coated cationic liposomes (125 mg total lipid/kg) via tail vain, respectively.

The antitumor activity was evaluated in terms of both tumor volume (mm^3) and survival (%). Tumor dimensions were determined at various time points using a caliper. Tumor volume (mm^3) was calculated using the following formula [23]:

$$\text{Tumor volume}\left(\text{mm}^3\right) = \left(a \times b^2\right)/2$$

where a is the length and b is the width in millimeters.

Median survival time (MST (day)) was defined as the time at which half of the mice had died. The percentage increased life span (ILS (%)) was calculated using the following equation [24,25]:

$$\text{ILS (\%)} = [(\text{MST of treated group} / \text{MST of control group}) - 1] \times 100$$

Body weight was measured simultaneously and was taken as a parameter of systemic toxicity.

2.7. In vivo tumor accumulation of DiI-labeled liposomes using in vivo fluorescence imaging

Approximately 5×10^5 of LLCC were inoculated subcutaneously in the flank region of C57BL/6 mice as described above. On day 8 after tumor inoculation (when the tumor volume reached values of 100–120 mm^3), mice were injected with 200 μl of DiI-labeled liposomes (125 mg lipid/kg) via the tail vein. At 6, 24 and 48 h post-injection, mice were anesthetized with isoflurane (FORANE, Abott Japan, Osaka, Japan), a short acting anesthetic, and maintained throughout the imaging process on a heating pad at 37 °C. Fluorescence imaging was performed with Fluorescence Image Analyzer LAS-4000IR (Fujifilm, Tokyo, Japan). The fluorescence images were acquired with a 1/8 s exposure time.

2.8. Determination of l-OHP amount in solid tumor

On day 8 after tumor inoculation, mice were injected intravenously with either l-OHP solution (5 mg/kg) or PEG-coated liposomal l-OHP formulations (5 mg l-OHP/kg, 125 mg total lipid/kg). At 6, 24 or 48 h post-injection, tumors were excised. Tumor tissues were digested according to the following procedure: the tissues were weighed, minced with scissors and placed in glass vials. Then 400 μl of 2 M KOH in isopropanol and 200 μl of H_2O_2 were added, and digestion proceeded by incubation at 65 °C for 12 h. The digested samples

were brought to 1.0 ml with 10% acetic acid and incubated at room temperature for a further 12 h. The content of l-OHP in the sample was then measured by atomic absorption photometry as described previously [10].

2.9. Statistical analysis

All values are expressed as mean ± S.D. Statistical analysis was performed with a two-tailed unpaired t test and one way ANOVA using Graphpad InStat software (GraphPad Software, CA, USA). The level of significance was set at $p < 0.05$.

3. Results

3.1. In vivo antitumor activity of l-OHP formulations

The antitumor activity of various l-OHP formulations in Lewis lung carcinoma cell (LLCC) bearing mice was evaluated (Fig. 1). Three sequential administrations with l-OHP formulations showed significant tumor growth suppression (Fig. 1A). The rank order of growth suppression was l-OHP in PEG-coated cationic liposomes >> l-OHP in PEG-coated neutral liposomes > free l-OHP in solution ($p < 0.001$, ANOVA). Little tumor growth suppression was observed in mice treated with empty PEG-coated cationic liposomes (no drug). The survival of treated mice are shown in Fig. 1B and the median survival time (MST) and percentage increased life span (ILS (%)) are summarized in Table 2. l-OHP formulations increased the survival of tumor-bearing mice compared with control and empty PEG-coated cationic liposome (no drug). Among the formulations, l-OHP containing PEG-coated cationic liposome showed the strongest effect on the survival of tumor-bearing mice; 50% of the mice (3 out of 6) became long-term survivors (>70 days) ($p < 0.001$). In addition, through the therapeutic experiment, no significant body weight loss was observed in any of the treated groups (data not shown). These results suggest that treatment with l-OHP containing PEG-coated cationic liposomes improves the MST of tumor-bearing mice without causing remarkable toxicity.

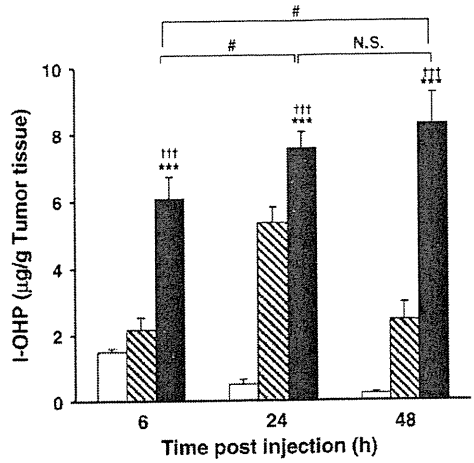

Fig. 3. In vivo tumor accumulation of l-OHP in LLCC-bearing mice. On day 8 after tumor inoculation, mice received an intravenous injection of l-OHP formulation at a dose of 5 mg l-OHP/kg. At 6, 24, or 48 h post injection, tumors were excised. The amount of l-OHP accumulated in tumor tissues was measured as platinum (Pt) using atomic absorption photometry. Open bars, hatched bars and closed bars represent free l-OHP solution, PEG-coated neutral liposomes and PEG-coated cationic liposomes, respectively. Data represent mean ± S.D ($n = 3$). $^{\dagger\dagger\dagger}p < 0.001$ against free l-OHP, $^{***}p < 0.01$ against PEG-coated neutral liposomes, $^{\#}p < 0.05$.

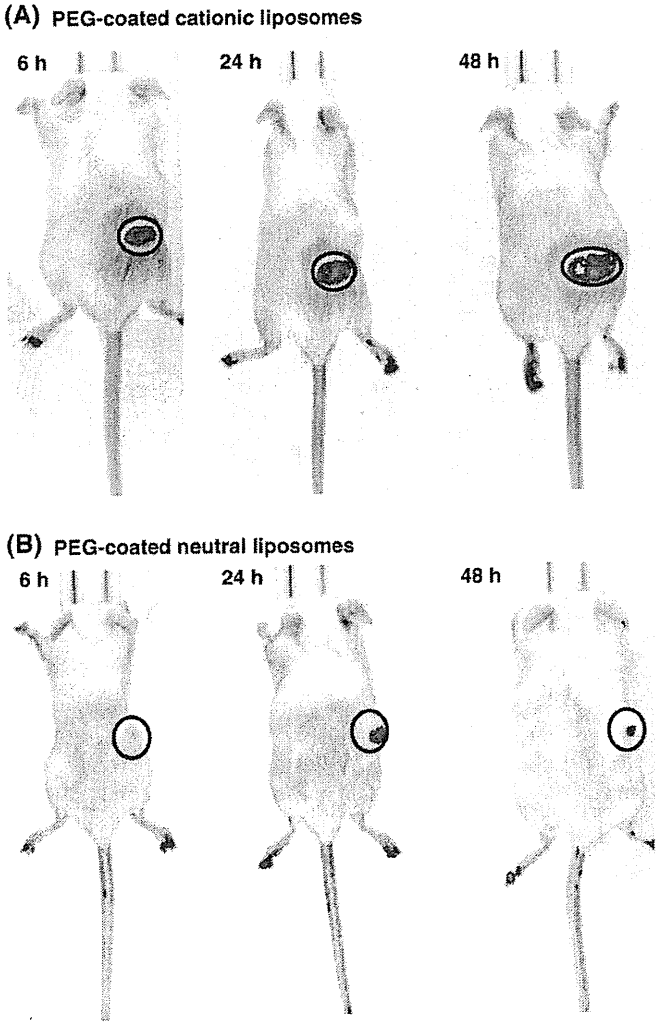

Fig. 2. In vivo tumor accumulation of fluorescently labeled PEG-coated liposomes. On day 8 after tumor inoculation mice received an intravenous injection of fluorescently (DiI) labeled empty PEG-coated liposomes (no drug) at a dose of 125 mg lipid/kg. At 6, 24, and 48 h post injection, in vivo optical images were taken. (A) PEG-coated cationic liposomes. (B) PEG-coated neutral liposomes. All fluorescence images were acquired with a 1/8 s exposure time. Circles indicate tumor locations, not exact tumor areas.

3.2. Accumulation of fluorescently (DiI)-labeled PEG-coated liposomes in solid tumor

Extensive and selective accumulation of drug carriers at the tumor site is essential for the success of in vivo drug targeting to solid tumors. To elucidate whether PEG-coated cationic liposomes accumulate substantially and selectively in a solid tumor than PEG-coated neutral liposomes, fluorescently (DiI)-labeled liposomes were intravenously administered and visualized in the tumor using an in vivo imaging system. Typical representative images are presented in Fig. 2. The fluorescence intensity distribution in the animals is presented in blue color on composite light/fluorescence images. PEG-coated cationic liposomes showed higher levels of accumulation in the tumor than PEG-coated neutral liposomes and accumulation was maintained at such high levels for an extended period (up to 48 h post injection). In addition, the pictures show a much broader area of distribution of PEG-coated cationic liposomes in the tumor region than PEG-coated neutral liposomes. These findings suggest that the PEG-coated cationic liposomes we recently developed [10], is a promising carrier for the achievement of tumor-targeted drug delivery.

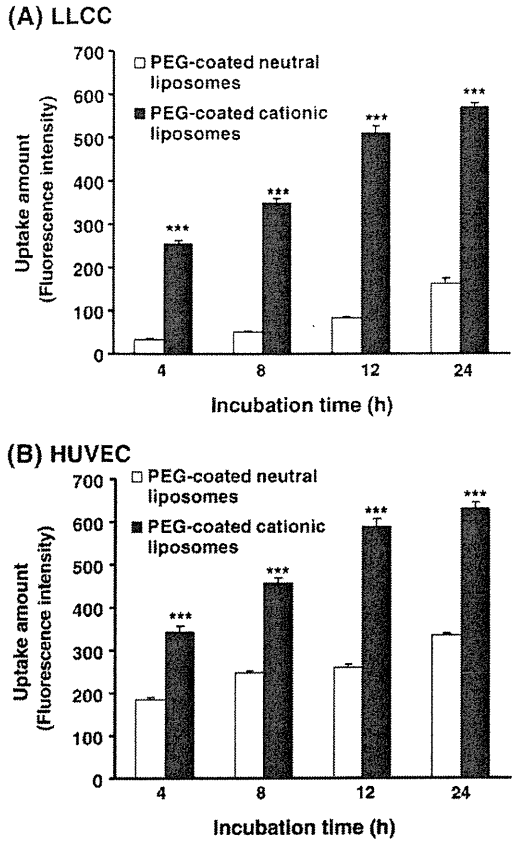

Fig. 4. Uptake of fluorescently labeled PEG-coated liposomes by LLCC and HUVEC. Cells (LLCC or HUVEC) were incubated with either DiI-labeled empty PEG-coated cationic liposomes or PEG-coated neutral liposomes. At 4, 8, 12 and 24 h post incubation, the cells were collected and the fluorescence of non internalized liposomes was quenched by incubating with 0.3% trypan blue solution. Then the cells were analyzed by flow cytometry. (A) LLCC. (B) HUVEC. Data represent the mean of three independent experiments ± S.D. ***$p < 0.001$ against PEG-coated neutral liposomes.

3.3. Accumulation of l-OHP in solid tumor

Mice bearing a LLCC solid tumor were treated with intravenous injection of either free l-OHP or liposomal l-OHP formulations to examine intra-tumoral l-OHP disposition (Fig. 3). Maximum intra-tumor accumulation of free l-OHP occurred at 6 h post-injection and gradually decreased to near zero levels by 48 h after injection. With PEG-coated neutral liposomes a 3-fold higher maximal l-OHP accumulation was achieved than with free l-OHP, but this value was reached only after 24 h, but at 48 h the level was still higher than the maximal level obtained with free 1-OHP. On the other hand, with PEG-coated cationic liposomes a 3-fold higher level of l-OHP was obtained after 6 h than with PEG-coated neutral liposomes while accumulation still increased up to 24 h and was sustained for at least another 24 h till 48 h post-injection.

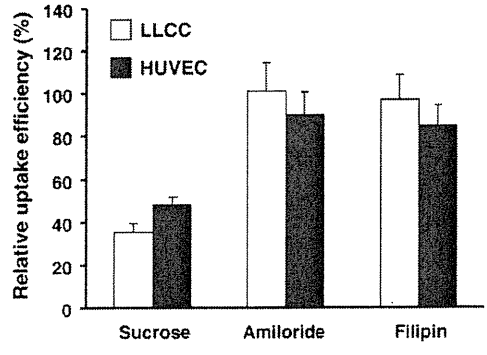

Fig. 5. Effects of inhibitors on cellular uptake of PEG-coated cationic liposomes. Cells (LLCC or HUVEC) were pre-incubated with various inhibitors for 30 min at 37 °C. Then fluorescently (DiI) labeled PEG-coated cationic liposomes (no drug) (4 μmol lipids/well) were added and the cells were further incubated for 1 h. After incubation the cells were collected and analyzed by flow cytometry following treatment with 0.3% trypan blue solution to quench fluorescence of extracellularly adhering non-internalized liposomes. Fluorescence intensity of DiI in untreated cells, representing the maximum internalized amount of PEG-coated cationic liposomes, was taken as 100%. Data represent mean ± S.D. ($n = 3$).

Table 3
In vitro cytotoxicity of various l-OHP formulations.

Formulation	IC_{50} (μM)	
	LLCC	HUVEC
Free l-OHP	7.9 ± 0.1	16.0 ± 1.0
PEG-coated cationic l-OHP liposomes	34.7 ± 0.9***	85.4 ± 5.7***
PEG-coated neutral l-OHP liposomes	115.4 ± 0.7***, †††	218.8 ± 8.0***, †††

Cells were incubated with media containing serial dilutions of various l-OHP formulations (free l-OHP, l-OHP containing PEG-coated cationic liposomes and l-OHP containing PEG-coated neutral liposomes). Following a 4-h incubation at 37 °C, the medium was replaced with fresh medium and incubated for a further 48 h. Then cell survival was determined by the MTT assay. Data represent mean ± S.D. ($n = 3$) ***$p < 0.001$ against free l-OHP, †††$p < 0.001$ against PEG-coated l-OHP neutral liposomes.

3.4. In vitro cellular uptake of fluorescently (DiI)-labeled PEG-coated liposomes

Fig. 4 shows that much larger amounts of PEG-coated cationic liposomes are internalized by both cell lines (LLCC and HUVEC) than of PEG-coated neutral liposomes. For both liposome formulations the amounts taken up gradually increased with time up to 24 h. In order to elucidate the uptake mechanism of the PEG-coated cationic liposomes, the effect of various endocytosis inhibitors on the uptake efficiency was investigated. Among the three inhibitors used (hypertonic sucrose, filipin and amiloride), only hypertonic sucrose extensively inhibited cellular uptake of PEG-coated cationic liposomes in both LLCC and HUVEC (Fig. 5). This indicates that the PEG-coated cationic liposomes are internalized by LLCC and HUVEC mainly via a clathrin-mediated endocytosis pathway.

3.5. Cytotoxicity of l-OHP formulations

The cytotoxicity of l-OHP formulations and empty PEG-coated cationic liposomes was investigated. As summarized in Table 3, for both LLCC and HUVEC, the IC_{50} value of l-OHP encapsulated in PEG-coated cationic liposome was much lower than that of l-OHP encapsulated in PEG-coated neutral liposome ($p < 0.001$). Both liposomal l-OHP formulations were significantly less cytotoxic in both cell lines than free l-OHP ($p < 0.001$). It appears that LLCC are more sensitive to l-OHP than HUVEC. In addition, empty PEG-coated cationic liposomes did not show any cytotoxicity at lipid concentrations corresponding to the l-OHP containing PEG-coated cationic liposomes we tested (not shown).

4. Discussion

We recently developed a PEG-coated cationic liposome and confirmed that such cationic liposome is a promising carrier delivering encapsulated chemotherapeutic agents to the tumor endothelium [10]. In addition, we showed that l-OHP containing PEG-coated cationic liposomes can bring about a potent anti-angiogenic effect in a mouse dorsal air sac (DAS) model [10]. Following up on these results, in the present study we aimed at investigating the antitumor effect of the l-OHP formulation in a murine tumor-xenograft model and providing an insight into the

probable mechanism of the enhanced antitumor effect of such l-OHP formulation.

An in vivo imaging study demonstrated a rapid accumulation and a more extensive intra-tumoral distribution of PEG-coated cationic liposomes in the solid tumor than of PEG-coated neutral liposomes (Fig. 2). Both PEG-coated liposomes, once administered in the blood stream, are expected to easily and efficiently gain access to the tumor tissue because of their prolonged circulation time in the blood compartment [14–16,26,27]. However, only PEG-coated cationic liposomes are able to selectively bind to endothelial cells in the tumor vasculature due to electrostatic interaction between the cationic surface charge of the liposome and negative charge of the plasma membrane of the endothelial cells as demonstrated earlier [10]. This notion was supported by our in vitro binding study using HUVEC, demonstrating that PEG-coated cationic liposomes massively associate with and are internalized by this endothelial cell line, regardless of the presence of PEG coating (Fig. 4B). Thurston et al. [11] also showed that cationic liposomes accumulate selectively in the vasculature of tumors, in contrast to anionic, neutral or PEG-coated neutral liposomes.

The in vivo imaging study also showed that the PEG-coated cationic liposomes are retained in the tumor tissue for a longer period than PEG-coated neutral liposomes (Fig. 2A). The continuous supply of PEG-coated cationic liposomes to the tumor tissue might saturate their binding sites on tumor vascular endothelial cells and thus facilitate their extravasation into the tumor interstitial space due to the EPR effect [17]. Upon diffusion into the interstitial space, the PEG-coated cationic liposomes are likely to bind to and subsequently to be internalized by the tumor cells as a result of electric interactions as shown in Figs. 4A and 5. This will result in prolonged retention time of the liposome in the tumor tissue (Fig. 2). Similar observations have been reported for PEG-coated liposomes modified with transferrin (Tf) [8,28,29]. On the other hand, PEG-coated neutral liposomes although also efficiently accumulating in the tumor tissue, albeit less rapidly than the cationic liposomes, are gradually eliminated from the tissue (Fig. 2). This is most likely explained by the lack of anchor (electric force) of the liposome preventing it from engaging in electrostatic interactions with endothelial cells and/or tumor cells (Fig. 4).

Quantitative determination of l-OHP in the tumor (Fig. 3) demonstrated that encapsulation in PEG-coated cationic liposomes causes l-OHP to rapidly accumulate and be retained in the tumor tissue, while PEG-coated neutral liposome resulted in slow l-OHP accumulation in and rapid elimination from the tissue. The accumulation patterns of l-OHP were very similar to those of the liposomes themselves, as visualized by the in vivo imaging system (Fig. 2). In addition, we recently reported that both liposomal l-OHP formulations retained 60–65% of encapsulated l-OHP in the presence of 50% mouse plasma following a 24-h incubation at 37 °C [10]. Accordingly, it was concluded, in terms of therapeutic efficacy, that PEG-coated cationic liposomes provide a superior efficiency in delivering l-OHP inside tumor tissue, thereby resulting in efficient tumor growth suppression and increased survival time of tumor bearing mice (Fig. 1 and Table 2). Generally, to obtain increased therapeutic efficacy, a drug carrier must achieve not only increased delivery of the drug in the tumor tissue but also enhanced interaction of the drug with and subsequent internalization by tumor cells. Although the exact mechanism by which the increased therapeutic efficacy in this study was obtained still is not clear, the results from our in vitro studies (Figs. 4 and 5 and Table 3) support the notion that, once accumulated in the tumor tissue, the PEG-coated cationic liposomes were presumably internalized by endothelial cells as well as tumor cells, and consequently delivered the encapsulated l-OHP in the cytoplasm of those cells. l-OHP, once delivered in the cytoplasm, would be retained for a long time (Fig. 3) due to the irreversible formation of complexes with proteins, DNA and other cellular macromolecules [30].

In contrast to cisplatin, l-OHP has no renal toxicity, only mild hematological and gastrointestinal toxicity, while neurotoxicity is dose-limiting [4,5]. The selective delivery of l-OHP to tumor tissues by the PEG-coated cationic liposome raises the possibility of reducing such toxicity. Actually, in this study, l-OHP containing PEG-coated cationic liposome did not show any remarkable side effect. Many studies have documented the specialization of the vasculature in tumors, both with respect to structural abnormalities and to potential molecular targets [31,32]. Cationic liposomes have been shown to associate readily with the endothelium of tumor vessels [11,33–38]. A recent study indicated that PEG-coated cationic liposomes associate with approximately 27 and 5% of vessel areas in tumors and normal tissues, respectively, in human and murine tumor models [39]. In our earlier study, we also observed a lack of selective accumulation/binding of the PEG-coated cationic liposomes to pre-existing blood vessels in the skin of the DAS model [10]. This points to an important difference in distribution of the liposomes between the vasculature of tumor tissue and that of normal tissues, which may be exploited while attempting to reduce the toxicity of l-OHP. Nevertheless, the cumulative toxicity of cationic liposomal anticancer drug formulations following several sequential administrations has not been evaluated yet. Further systemic experiments following long-term treatments with our l-OHP formulation are currently underway in our laboratory.

Recent efforts have focused on the application of various combination treatment regimens that include cytotoxic and anti-angiogenic agents, to improve the overall antitumor response in preclinical models in vivo [40]. However, preclinical and clinical studies have indicated that the toxicity profile of such combinations differs from that of conventional single chemotherapy, thus ruling out additive toxicity as a major limitation of the combination chemotherapy [41,42]. In this study, we demonstrated that l-OHP containing PEG-coated cationic liposomes exert their efficient antitumor activity probably via a dual targeting approach, addressing not only the tumor endothelium but also the tumor cells. A dual mechanism of action has been proposed by Pastorino et al. [18,19]: indirect tumor cell kill via the destruction of tumor endothelium by doxorubicin (DXR)-containing liposomes targeted to aminopeptidase N (NGR-targeted DXR liposomes) and direct tumor cell kill via delivery of liposomal DXR to the tumor interstitial space. Such dual targeting approach, vascular-targeting and tumor-targeting with a single liposomal anticancer drug formulation, may have strong potential to overcome some major limitations in conventional anticancer chemotherapy.

5. Conclusion

In this study, we showed that with l-OHP containing PEG-coated cationic liposomes a remarkable tumor growth suppression and increased survival time of tumor-bearing mice can be achieved, without apparent side effects, presumably as a result of delivering the encapsulated drug to both blood vessels located specifically at tumor sites and to the tumor cells themselves. The dual targeting approach, vascular-targeting and tumor-targeting with a single liposomal anticancer drug formulation, may have the potential to overcome some of the major shortcomings of conventional chemotherapeutic strategies.

Acknowledgments

We thank Dr. G.L. Scherphof for his helpful advice in preparing this manuscript. This study was supported, in part, by the Kobayashi Fund for Cancer Research and the Knowledge Cluster Initiative from Ministry of Education, Science and Technology.

References

[1] A. Ibrahim, S. Hirschfeld, M.H. Cohen, D.J. Griebel, G.A. Williams, R. Pazdur, FDA drug approval summaries: oxaliplatin, Oncologist 9 (2004) 8–12.
[2] C. Tournigand, T. Andre, E. Achille, G. Lledo, M. Flesh, D. Mery-Mignard, E. Quinaux, C. Couteau, M. Buyse, G. Ganem, B. Landi, P. Colin, C. Louvet, A. de Gramont, FOLFIRI

followed by FOLFOX6 or the reverse sequence in advanced colorectal cancer: a randomized GERCOR study, J. Clin. Oncol. 22 (2004) 229–237.
[3] A. Pessino, A. Sobrero, Optimal treatment of metastatic colorectal cancer, Expert Rev. Anticancer Ther. 6 (2006) 801–812.
[4] A. Grothey, Oxaliplatin-safety profile: neurotoxicity, Semin. Oncol. 30 (2003) 5–13.
[5] A. Pietrangeli, M. Leandri, E. Terzoli, B. Jandolo, C. Garufi, Persistence of high-dose oxaliplatin-induced neuropathy at long-term follow-up, Eur. Neurol. 56 (2006) 13–16.
[6] L. Pendyala, P.J. Creaven, In vitro cytotoxicity, protein binding, red blood cell partitioning, and biotransformation of oxaliplatin, Cancer Res. 53 (1993) 5970–5976.
[7] H. Cabral, N. Nishiyama, K. Kataoka, Optimization of (1,2-diamino-cyclohexane) platinum(II)-loaded polymeric micelles directed to improved tumor targeting and enhanced antitumor activity, J. Control. Release 121 (2007) 146–155.
[8] R. Suzuki, T. Takizawa, Y. Kuwata, M. Mutoh, N. Ishiguro, N. Utoguchi, A. Shinohara, M. Eriguchi, H. Yanagie, K. Maruyama, Effective anti-tumor activity of oxaliplatin encapsulated in transferrin-PEG-liposome, Int. J. Pharm. 346 (2008) 143–150.
[9] G.P. Stathopoulos, T. Boulikas, A. Kourvetaris, J. Stathopoulos, Liposomal oxaliplatin in the treatment of advanced cancer: a phase I study, Anticancer Res. 26 (2006) 1489–1493.
[10] A. Abu-Lila, T. Suzuki, Y. Doi, T. Ishida, H. Kiwada, Oxalipalatin targeting to angiogenic vessels by PEGylated cationic liposomes suppresses the angiogenesis in a dosal air sac model, J. Control. Release 134 (2009) 18–25.
[11] G. Thurston, J.W. McLean, M. Rizen, P. Baluk, A. Haskell, T.J. Murphy, D. Hanahan, D.M. McDonald, Cationic liposomes target angiogenic endothelial cells in tumors and chronic inflammation in mice, J. Clin. Invest. 101 (1998) 1401–1413.
[12] T. Nomura, N. Koreeda, F. Yamashita, Y. Takakura, M. Hashida, Effect of particle size and charge on the disposition of lipid carriers after intratumoral injection into tissue-isolated tumors, Pharm. Res. 15 (1998) 128–132.
[13] J. Wu, A. Lee, Y. Lu, R.J. Lee, Vascular targeting of doxorubicin using cationic liposomes, Int. J. Pharm. 337 (2007) 329–335.
[14] T.M. Allen, C. Hansen, F. Martin, C. Redemann, A. Yau-Young, Liposomes containing synthetic lipid derivatives of poly(ethylene glycol) show prolonged circulation half-lives in vivo, Biochim. Biophys. Acta 1066 (1991) 29–36.
[15] C. Allen, N. Dos Santos, R. Gallagher, G.N. Chiu, Y. Shu, W.M. Li, S.A. Johnstone, A.S. Janoff, L.D. Mayer, M.S. Webb, M.B. Bally, Controlling the physical behavior and biological performance of liposome formulations through use of surface grafted poly(ethylene glycol), Biosci. Rep. 22 (2002) 225–250.
[16] A.L. Klibanov, K. Maruyama, A.M. Beckerleg, V.P. Torchilin, L. Huang, Activity of amphipathic poly(ethylene glycol) 5000 to prolong the circulation time of liposomes depends on the liposome size and is unfavorable for immunoliposome binding to target, Biochim. Biophys. Acta 1062 (1991) 142–148.
[17] Y. Matsumura, H. Maeda, A new concept for macromolecular therapeutics in cancer chemotherapy: mechanism of tumoritropic accumulation of proteins and the antitumor agent smancs, Cancer Res. 46 (1986) 6387–6392.
[18] F. Pastorino, C. Brignole, D. Marimpietri, M. Cilli, C. Gambini, D. Ribatti, R. Longhi, T.M. Allen, A. Corti, M. Ponzoni, Vascular damage and anti-angiogenic effects of tumor vessel-targeted liposomal chemotherapy, Cancer Res. 63 (2003) 7400–7409.
[19] F. Pastorino, C. Brignole, D. Di Paolo, B. Nico, A. Pezzolo, D. Marimpietri, G. Pagnan, F. Piccardi, M. Cilli, R. Longhi, D. Ribatti, A. Corti, T.M. Allen, M. Ponzoni, Targeting liposomal chemotherapy via both tumor cell-specific and tumor vasculature-specific ligands potentiates therapeutic efficacy, Cancer Res. 66 (2006) 10073–10082.
[20] G.R. Bartlett, Colorimetric assay methods for free and phosphorylated glyceric acids, J. Biol. Chem. 234 (1959) 469–471.
[21] T.C. Stover, Y.S. Kim, T.L. Lowe, M. Kester, Thermoresponsive and biodegradable linear-dendritic nanoparticles for targeted and sustained release of a pro-apoptotic drug, Biomaterials 29 (2008) 359–369.
[22] K. Atobe, T. Ishida, E. Ishida, K. Hashimoto, H. Kobayashi, J. Yasuda, T. Aoki, K. Obata, H. Kikuchi, H. Akita, T. Asai, H. Harashima, N. Oku, H. Kiwada, In vitro efficacy of a sterically stabilized immunoliposomes targeted to membrane type 1 matrix metalloproteinase (MT1-MMP), Biol. Pharm. Bull. 30 (2007) 972–978.
[23] J.H. Kim, Y.S. Kim, K. Park, S. Lee, H.Y. Nam, K.H. Min, H.G. Jo, J.H. Park, K. Choi, S.Y. Jeong, R.W. Park, I.S. Kim, K. Kim, I.C. Kwon, Antitumor efficacy of cisplatin-loaded glycol chitosan nanoparticles in tumor-bearing mice, J. Control. Release 127 (2008) 41–49.
[24] M.R. Kviecinski, K.B. Felipe, T. Schoenfelder, L.P. de Lemos Wiese, M.H. Rossi, E. Goncalez, J.D. Felicio, D.W. Filho, R.C. Pedrosa, Study of the antitumor potential of *Bidens pilosa* (Asteraceae) used in Brazilian folk medicine, J. Ethnopharmacol. 117 (2008) 69–75.
[25] D.E. Lopes de Menezes, L.M. Pilarski, A.R. Belch, T.M. Allen, Selective targeting of immunoliposomal doxorubicin against human multiple myeloma in vitro and ex vivo, Biochim. Biophys. Acta 1466 (2000) 205–220.
[26] K. Kawahara, A. Sekiguchi, E. Kiyoki, T. Ueda, K. Shimamura, Y. Kurosaki, S. Miyaoka, H. Okabe, M. Miyajima, J. Kimura, Effect of TRX-liposomes size on their prolonged circulation in rats, Chem. Pharm. Bull. (Tokyo) 51 (2003) 336–338.
[27] K. Morimoto, M. Kondo, K. Kawahara, H. Ushijima, Y. Tomino, M. Miyajima, J. Kimura, Advances in targeting drug delivery to glomerular mesangial cells by long circulating cationic liposomes for the treatment of glomerulonephritis, Pharm. Res. 24 (2007) 946–954.
[28] O. Ishida, K. Maruyama, H. Tanahashi, M. Iwatsuru, K. Sasaki, M. Eriguchi, H. Yanagie, Liposomes bearing polyethyleneglycol-coupled transferrin with intracellular targeting property to the solid tumors in vivo, Pharm. Res. 18 (2001) 1042–1048.
[29] S. Sofou, G. Sgouros, Antibody-targeted liposomes in cancer therapy and imaging, Expert Opin. Drug Deliv. 5 (2008) 189–204.
[30] M.A. Graham, G.F. Lockwood, D. Greenslade, S. Brienza, M. Bayssas, E. Gamelin, Clinical pharmacokinetics of oxaliplatin: a critical review, Clin. Cancer Res. 6 (2000) 1205–1218.
[31] D. Fukumura, R.K. Jain, Tumor microvasculature and microenvironment: targets for anti-angiogenesis and normalization, Microvasc. Res. 74 (2007) 72–84.
[32] D. Fukumura, R.K. Jain, Tumor microenvironment abnormalities: causes, consequences, and strategies to normalize, J. Cell. Biochem. 101 (2007) 937–949.
[33] R.B. Campbell, D. Fukumura, E.B. Brown, L.M. Mazzola, Y. Izumi, R.K. Jain, V.P. Torchilin, L.L. Munn, Cationic charge determines the distribution of liposomes between the vascular and extravascular compartments of tumors, Cancer Res. 62 (2002) 6831–6836.
[34] R.B. Campbell, B. Ying, G.M. Kuesters, R. Hemphill, Fighting cancer: from the bench to bedside using second generation cationic liposomal therapeutics, J. Pharm. Sci. 98 (2009) 411–429.
[35] S. Strieth, M.E. Eichhorn, A. Werner, B. Sauer, M. Teifel, U. Michaelis, A. Berghaus, M. Dellian, Paclitaxel encapsulated in cationic liposomes increases tumor microvessel leakiness and improves therapeutic efficacy in combination with cisplatin, Clin. Cancer Res. 14 (2008) 4603–4611.
[36] S. Strieth, C.F. Nussbaum, M.E. Eichhorn, M. Fuhrmann, M. Teifel, U. Michaelis, A. Berghaus, M. Dellian, Tumor-selective vessel occlusions by platelets after vascular targeting chemotherapy using paclitaxel encapsulated in cationic liposomes, Int. J. Cancer 122 (2008) 452–460.
[37] C.R. Dass, P.F. Choong, Selective gene delivery for cancer therapy using cationic liposomes: in vivo proof of applicability, J. Control. Release 113 (2006) 155–163.
[38] C.R. Dass, P.F. Choong, Targeting of small molecule anticancer drugs to the tumour and its vasculature using cationic liposomes: lessons from gene therapy, Cancer Cell Int. 6 (2006) 17.
[39] A.V. Kalra, R.B. Campbell, Development of 5-FU and doxorubicin-loaded cationic liposomes against human pancreatic cancer: implications for tumor vascular targeting, Pharm. Res. 23 (2006) 2809–2817.
[40] S. Ghosh, P. Maity, Augmented antitumor effects of combination therapy with VEGF antibody and cisplatin on murine B16F10 melanoma cells, Int. Immunopharmacol. 7 (2007) 1598–1608.
[41] M. Martinelli, K. Bonezzi, E. Riccardi, E. Kuhn, R. Frapolli, M. Zucchetti, A.J. Ryan, G. Taraboletti, R. Giavazzi, Sequence dependent antitumour efficacy of the vascular disrupting agent ZD6126 in combination with paclitaxel, Br. J. Cancer 97 (2007) 888–894.
[42] J.J. Knox, D. Hedley, A. Oza, R. Feld, L.L. Siu, E. Chen, M. Nematollahi, G.R. Pond, J. Zhang, M.J. Moore, Combining gemcitabine and capecitabine in patients with advanced biliary cancer: a phase II trial, J. Clin. Oncol. 23 (2005) 2332–2338.

Journal of Controlled Release 137 (2009) 234–240

Contents lists available at ScienceDirect

Journal of Controlled Release

journal homepage: www.elsevier.com/locate/jconrel

Effect of siRNA in PEG-coated siRNA-lipoplex on anti-PEG IgM production

Tatsuaki Tagami, Kazuya Nakamura, Taro Shimizu, Tatsuhiro Ishida, Hiroshi Kiwada *

Department of Pharmacokinetics and Biopharmaceutics, Subdivision of Biopharmaceutical Sciences, Institute of Health Biosciences, The University of Tokushima, 1-78-1, Sho-machi, Tokushima 770-8505, Japan

ARTICLE INFO

Article history:
Received 31 July 2008
Accepted 4 April 2009
Available online 8 April 2009

Keywords:
Accelerated blood clearance (ABC) phenomenon
Polyethylene glycol (PEG)
Anti-PEG IgM
PEG-coated siRNA/cationic liposome complex (PSCL)
Small interfering RNA (siRNA)

ABSTRACT

For efficient delivery of small interfering RNA (siRNA) *in vivo*, it is important to control the blood circulation of the delivery vehicle. Surface modification of the siRNA/cationic liposome complex (siRNA-lipoplex) with polyethylene glycol (PEG) is expected to enhance circulation time in blood. However, we have recently reported that anti-PEG IgM production after the first injection of PEG-coated liposome is responsible for a reduction in the blood circulation of the second dose of the liposome, which is known as the accelerated blood clearance (ABC) phenomenon. It is unknown whether a PEG-coated siRNA-lipoplex (PSCL) can cause the ABC phenomenon and anti-PEG IgM production. In this study, an anti-PEG IgM response to PSCL was detected and was inversely related to the PSCL dose. Interestingly, the anti-PEG IgM response was significantly lower for PSCL than it was for PEG-coated naked cationic liposomes (PCL). The studies with splenectomized mice and nude mice indicated that anti-PEG IgM production was closely related to an interaction of PSCL and PCL with the spleen, which is associated with a T cell-independent mechanism. In addition, PSCL induced apoptosis on IgM-expressing splenic cells more strongly than PCL did, which suggests that accumulation in the spleen and the apoptotic effect of PEG-coated substances on splenic B cells could affect the potency of anti-PEG IgM production.

1. Introduction

A small interfering RNA (siRNA) has sequence-specific and potent gene silencing properties based on an RNA interference mechanism for molecular-targeted drugs [1]. A growing number of studies have used siRNAs as potential therapeutic agents for treating numerous diseases, including cancer and genetic or viral infections [2,3]. The therapeutic application of siRNA is largely dependent on the development of a delivery vehicle and such a vehicle must be applied efficiently, safely and repeatedly. Cationic liposome is candidate that is expected to satisfy these requirements [4]. However, the use of a siRNA/cationic liposome complex (siRNA-lipoplex), such as systemic delivery in a clinical situation, is questionable due to poor blood circulation characteristics. Therefore, the surface of siRNA-lipoplex is frequently modified by polyethylene glycol (PEG)-conjugated lipid (PEGylation). PEGylation extends circulation time for liposomes, the mechanism of which is hypothesized to be as follows: the PEG on the liposomal surface attracts a water shell, resulting in the reduced adsorption of opsonins and the recognition of liposome by the cells of a mononuclear phagocyte system (MPS) [5,6]. The technology of PEG-coated liposomes is utilized for anti-cancer drugs in clinical settings [7]. The PEGylation of siRNA-lipoplexes may also enhance the circulation time of the complex and can increase the amount of siRNA in the targeted tissue, which offers significant potential for developing siRNA-based therapy, particularly for the application of systemic administration.

However, we and other researchers have reported that an intravenous injection of PEG-coated liposomes causes a second dose of PEG-coated liposomes, injected a few days later, to lose its long-circulating characteristics and to accumulate extensively in the liver [8,9], which is known as the "accelerated blood clearance (ABC) phenomenon." On the basis of our recent results [10,11], we proposed the following tentative mechanism for the cause of this phenomenon: anti-PEG IgM, which is produced in the spleen in response to a first dose, selectively binds to the PEG of the second dose liposomes injected several days later and subsequently activates the complement system. This, in turn, leads to opsonization of the second dose of liposome by C3 fragments and, as a consequence, to enhanced uptake of the liposomes by the Kupffer cells in the liver. In addition, we recently reported that the immune response to PEG on the liposome surface happens in a T cell-independent (TI) manner [12].

The ABC phenomenon involving anti-PEG IgM production can also be an important factor in designing an efficient delivery system of genes or nucleic acids. In an early study, it was reported that PEG-coated lipid nano-particles encapsulating plasmid DNA (pDNA) greatly enhances anti-PEG IgM production compared with PEG-coated nano-particles without pDNA. Consequently, pDNA expression declined highly in tumor tissue following its second injection [13].

* Corresponding author. Tel.: +81 88 633 7259; fax: +81 88 633 7260.
E-mail address: hkiwada@ph.tokushima-u.ac.jp (H. Kiwada).

0168-3659/$ – see front matter © 2009 Elsevier B.V. All rights reserved.
doi:10.1016/j.jconrel.2009.04.006

siRNA and pDNA also are well known as potent inducers of interferon and inflammatory cytokine when formulated with a lipid- or polycation-based delivery system [14,15]. For these reasons, we assumed that siRNA entrapped in PEG-coated cationic liposome affects the anti-PEG IgM response caused by the first dose of PSCL. In this study, therefore, we investigated the effect of siRNA in the PSCL on anti-PEG IgM production and the contribution of spleen and splenic B cells to the anti-PEG IgM responses caused by first PSCL dose.

2. Materials and methods

2.1. Materials

2-distearoyl-*sn*-glycero-3-phosphoethanolamine-*n*-[methoxy (polyethylene glycol)-2000 ($mPEG_{2000}$-DSPE), 1-palmitoyl-2-oleoyl-*sn*-glycero-3-phosphocholine (POPC) and dioleoylphospatidylethanolamine (DOPE) were generously donated by NOF (Tokyo, Japan). O,O′-ditetradecanoyl-N-(α-trimethyl ammonio acetyl) diethanolamine chloride (DC-6-14) as cationic lipid was purchased from Sogo Pharmaceutical (Tokyo, Japan). Cholesterol (CHOL) was of analytical grade (Wako Pure Chemical, Osaka, Japan). All lipids were used without further purification. ^{3}H-Cholesterylhexadecyl ether (^{3}H-CHE) was purchased from PerkinElmer Life Science (MA, USA). All other reagents were of analytical grade.

2.2. siRNA

siRNA, chemically synthesized and purified by HPLC, was purchased from Nippon EGT (Toyama, Japan). The sequence of siRNA for GFP, which does not have a target gene in mice, is as follows: sense sequence, 5′-GGC UAC GUC CAG GAG CGC ATT-3′; and, antisense sequence, 5′-UGC GCU CCU GGA CGU AGC CTT-3′. siRNA was dissolved in RNase free water at a final concentration of 50 μM.

2.3. Animals

Male Std-ddY mice aged 4–5 weeks (20–25 g), male BALB/cCr Slc mice aged 4–5 weeks (20–25 g), and male BALB/c Slc-nu/nu mice aged 5–6 weeks (20–25 g), were purchased from Japan SLC (Shizuoka, Japan). Mice were maintained under pathogen-free conditions. All animal experiments were evaluated and approved by the Animal and Ethics Review Committee of the University of Tokushima.

2.4. Preparation of cationic liposome

Cationic liposome was composed of DC-6-14:POPC:CHOL:DOPE (10:30:30:30, molar ratio). Liposome was prepared as previously described [12]. Briefly, the lipids were dissolved in chloroform. After evaporation of the organic solvent, the resulting lipid film was hydrated in 9% sucrose to produce multilamellar vesicles (MLVs). The MLVs were sized by repeated extrusion thorough polycarbonate membrane filters (Nucleopore, CA, USA) with consecutive pore size of 400, 200 and 100 nm. The mean diameters and zeta potentials of the resulting liposomes were determined using a NICOMP 370 HPL submicron particle analyzer (Particle Sizing System, CA, USA). The mean diameter and zeta potential for cationic liposome were 90.7 ± 2.3 nm and 18.5 ± 0.5 mV ($n = 3$), respectively. The lipid content of the liposomes was determined using a cholesterol E-test Wako kit (Wako Pure Chemical, Osaka, Japan).

2.5. Preparation of PEG-coated siRNA-lipoplex and PEG-coated cationic liposome

For the formulation of siRNA-lipoplex, for instance, siRNA (12.5 μg) and cationic liposome (0.625 μmol, phospholipids) were mixed and incubated for 20 min at room temperature. For PEGylation of siRNA-lipoplex and cationic liposome to produce PEG-coated siRNA-lipoplex (PSCL) and PEG-coated cationic liposome (PCL), a post-insertion technique was used [16]. Briefly, $mPEG_{2000}$-DSPE (5 mol% of total lipid) in 9% sucrose solution and siRNA-lipoplex or cationic liposome was mixed. The mixture was vortexed for 15 s and gently shaken for 1 h at 37 °C. The mean diameters were 205.4 ± 5.2 nm for PSCLs ($n = 3$) and 100.1 ± 3.9 nm for PCLs ($n = 3$). The mean zeta potentials were 9.0 ± 1.7 mV for PSCLs ($n = 3$) and 10.2 ± 1.2 mV for PCLs ($n = 3$). To check the presence of free siRNA in the prepared PSCL, electrophoresis was carried out with 2% Agarose gel. No bands relating free siRNA were detected, indicating that almost 100% of the siRNA was associated with and/or encapsulated in PEG-coated cationic liposome. In addition, to study RNase resistance of PSCL, PSCLs were incubated in 50% fetal bovine serum for 30 min at 37 °C. Then, the fragmentation of siRNA or released siRNA was determined using electrophoresis. No fragment of digested siRNA or released siRNA was detected. To determine the biodistribution of PCLs and PSCLs, the liposomes were labeled with a trace amount of ^{3}H-CHE (40 μCi/μmol of phospholipids) as a nonexchangeable lipid phase marker.

2.6. Splenic clearance of single injection

^{3}H-CHE labeled PSCL or ^{3}H-CHE labeled PCL (0.625 μmol phospholipids/mouse) were intravenously injected into mice via the tail vein. At selected post-injection time points (2 min, 15 min, 30 min, 1 h, 2 h, 4 h, 8 h or 24 h), the mice were euthanized. Blood samples were then obtained by heart puncture, and spleens were collected from the mice after withdrawing the blood samples. Radioactivity in spleen tissues was assayed as described previously [17]. Pharmacokinetic parameters were calculated using polyexponential curve fitting and the least-squares parameter estimation program SAAM II (Micromath, UT, USA).

The splenic clearance (CLs) was calculated as follows:

$$CLs = X_{(24)} / AUC_{(0\rightarrow 24)}.$$

Where $X_{(24)}$ (%Dose) is the amount of PSCLs or PCLs accumulated in spleen at 24 h post-injection. $AUC_{(0\rightarrow 24)}$ (%Dose·h/ml) is the area under the blood concentration-time curve from time 0 to 24 h post-injection.

2.7. Blood clearance and hepatic clearance of second injection (test liposome)

For pretreatment (first dose), either PSCL (0.625 μmol phospholipids and 12.5 μg siRNA/mouse) or PCL (0.625 μmol phospholipids/mouse) was intravenously injected into mice via the tail vein. To determine the biodistribution of the second dose, ^{3}H-CHE labeled PCL (test liposome, 0.625 μmol phospholipids/mouse) was intravenously injected into the mice via the tail vein at day 5 after the first injection. At selected post-injection time points (2 min, 15 min, 30 min, 1 h, 2 h, 4 h, 8 h or 24 h), the mice were euthanized. Blood samples were then obtained by heart puncture, and livers were collected from the mice after withdrawing the blood samples. Mice that were pretreated with 9% sucrose served as controls. Radioactivity in the blood and liver was assayed as described previously [17]. Pharmacokinetic parameters were calculated and the key parameters were obtained using polyexponential curve fitting and the least-squares parameter estimation program SAAM II.

The hepatic clearance (CLh) was calculated as follows:

$$CLh = X_{(24)} / AUC_{(0\rightarrow 24)}$$

Where $X_{(24)}$ (%Dose) is the amount of test liposomes accumulated in liver at 24 h post-injection. $AUC_{(0\rightarrow 24)}$ (%Dose·h/ml) is the area under the blood concentration-time curve from time 0 to 24 h post-injection.

2.8. Detection of IgM and IgG against PEG

A simple ELISA procedure as described before [12] was employed to detect IgM or IgG against PEG in the serum. Briefly, 10 nmol of $mPEG_{2000}$-DSPE in 50 μl ethanol was added to a 96-well plate. Lipid-coated plates were allowed to air dry completely for 2 h. The plates were then blocked for 1 h with Tris-buffered saline containing 1% BSA and were subsequently washed. Diluted serum samples (1:100) (100 μl) were then applied in appointed wells, incubated for 1 h and washed three times. Horseradish peroxidase (HRP)-conjugated antibody (100 μl, 1 μg/ml, Goat anti-mouse IgM (or IgG) IgG-HRP conjugate (Bethyl Laboratories, TX, USA)) was added to the wells. After incubation for 1 h, the wells were washed. ELISA activity was measured at 490 nm using a Microplate reader (Wallac1420 ARVOsx, PerkinElmer Life Science, MA, USA). All incubations were performed at room temperature.

2.9. Splenectomy

Splenectomy was carried out according to a method described earlier [10]. Briefly, after shaving the skin, a 2-cm incision was made in the skin of anaesthetized mice on the left flank. The peritoneal membrane was opened, and the entire spleen was removed after ligating the splenic vein and artery at the hilum. The peritoneal membrane and the skin were closed separately with surgical silk-thread. This procedure ensured that the spleen was removed in total and that no splenic fragments were left behind, as confirmed by examining the mice at the time of death. For sham-operated mice, the skin and peritoneal membrane were surgically opened and closed. One day (24 h) after surgery, either PSCLs or PCLs were injected into mice and blood samples were withdrawn on day 5 after injection. The detection of anti-PEG IgM in the sample was performed using ELISA, as described above.

2.10. Detection of apoptosis of IgM-expressing B cells in spleen

At 24 h post-injection of either PSCLs or PCLs, spleen tissues were removed from the mice under anaesthetization. As a positive control, an anti-cancer drug, doxorubicin solution (200 μg/mouse, approximately 8 mg/kg; Sigma, MO, USA), was intravenously injected. Spleen cell suspension was prepared using a Cell Strainer (100 μm, Becton Dickinson, NJ, USA) as described previously [12]. The apoptosis of splenic cells was detected using an "*in situ* cell death detection kit, Fluorescein" (Roche Diagnostics, Mannheim, Germany) according to the protocol manufacture recommended with minor modifications. To gate IgM-expressing B cells, cells were then incubated with Alexa Fluor 647 goat anti-mouse IgM (Invitrogen, CA, USA) for 1 h at room temperature. Cells were washed and then analyzed by flow cytometer (Guava EasyCyte Mini, GE Healthcare, CA, USA). In each sample, 30,000 cells were counted. Data analysis was performed using CytoSoft software (GE Healthcare).

2.11. Statistical analysis

All values are expressed as the mean ± S.D. Statistical analysis was performed with a two-tailed unpaired Student's *t* test using GraphPad InStat software (GraphPad Software, CA, USA). The level of significance was set at $p<0.05$.

3. Results

3.1. Dose dependency of PSCL or PCL on anti-PEG IgM production

We recently reported evidence indicating that anti-PEG IgM production after the first injection of PEG-coated empty liposome is responsible for the ABC phenomenon [11,12]. In the present study, to investigate the effect of siRNA in the PEG-coated siRNA lipoplex (PSCL) on anti-PEG IgM production, various doses of either PSCL or PCL were intravenously injected into mice. Anti-PEG IgM responses in serum were assessed on day 5 after the injection, which remarkably detected the induction of the ABC phenomenon, as in our previous report [11]. Anti-PEG IgM responses to PSCL and PCL showed a similar tendency (Fig. 1). Both anti-PEG IgM responses were reduced as their doses increased, and the responses were completely inhibited at higher dose (5 μmol phospholipids/mouse). Interestingly, at doses of 0.3125, 0.625 and 1.25 μmol phospholipids/mouse, anti-PEG IgM responses to PSCL were significantly lower than the responses to PCL.

To investigate whether the produced anti-PEG IgM accelerated clearance of the second dose, ^{3}H-CHE-labeled PCL (test liposome) was injected at day 5 after either PSCL (0.625 μmol phospholipids and 12.5 μg siRNA/mouse), PCL (0.625 μmol phospholipids/mouse) or 9% sucrose (control) was given. The blood concentration profile and calculated hepatic clearance (CLh) value are shown in Fig. 2. The test liposome showed a long-circulating characteristic in control mice ($T_{1/2}=12.4$ h) and a lower hepatic clearance value. In the mice pretreated with PCL, the test liposome cleared rapidly and completely disappeared from the blood within 24 h ($T_{1/2}=3.4$ h). Concomitantly, the CLh of test liposomes was increased by 10.2-fold compared with the control value. In the mice treated with PSCL, test liposome cleared rapidly from blood circulation, but the rate was moderate compared to that in the mice treated with PCL ($T_{1/2}=7.8$ h). Hepatic clearance was increased 4.6-fold compared to the control values.

3.2. Time course of changes in anti-PEG IgM or anti-PEG IgG responses

Then we investigated anti-PEG IgM and IgG responses as a function of time following injection with fixed doses (PSCL, 0.625 μmol phospholipids and 12.5 μg siRNA per mouse, approximately 25 μmol phospholipids and 500 μg siRNA per kg of body weight; PCL, 0.625 μmol phospholipids per mouse, approximately 25 μmol phospholipids per kg of body weight). As shown in Fig. 3, anti-PEG IgM responses were relatively higher than anti-PEG IgG responses, but a simultaneous tendency of anti-PEG IgM and anti-PEG IgG responses was generally observed the day after the injection of PSCL and PCL. Anti-PEG IgM and IgG responses were first detected at day 3 after the injection, reached the maximum at day 5, then decreased gradually

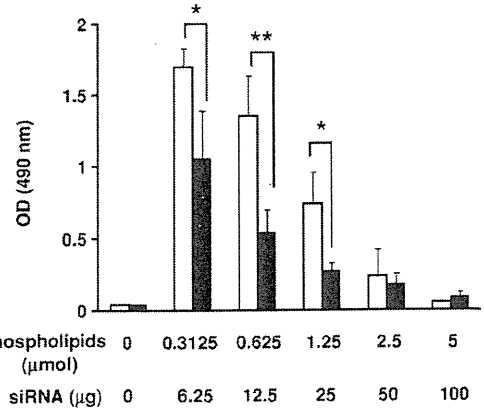

Fig. 1. Dose-response effect on the anti-PEG IgM response in mice. Various doses of either PSCL (0, 0.3125, 0.625, 1.25, 2.5 and 5 μmol phospholipids and 0, 6.25, 12.5, 25, 50 and 100 μg siRNA/mouse, respectively) or PCL (0, 0.3125, 0.625, 1.25, 2.5 and 5 μmol phospholipids/mouse) were intravenously injected into ddY mice. Five day later, blood was withdrawn and serum was collected. The sera collected from the naïve mice were used as the control (dose 0). Anti-PEG IgM was detected with ELISA as described in the Materials and methods section. □, PCL; ■, PSCL. Each value represents the mean ± S.D. ($n=4$). * $p<0.05$, ** $p<0.01$.

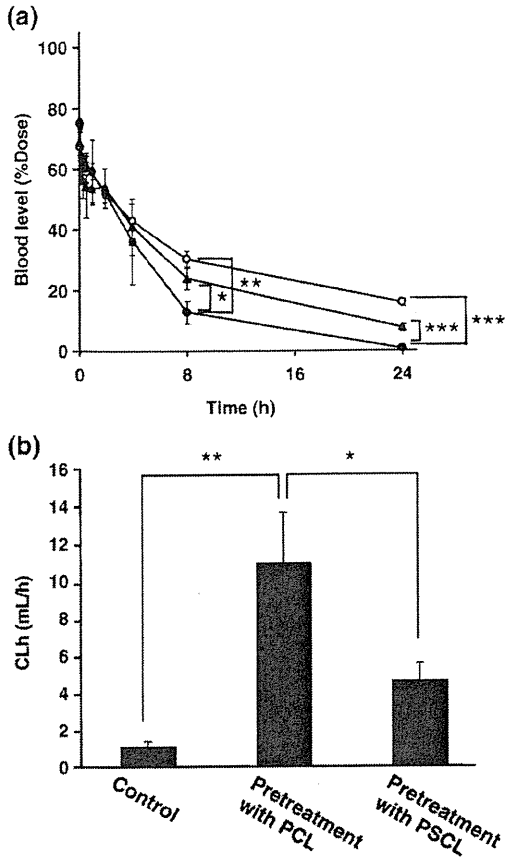

Fig. 2. Effect of the first dose of PSCL and PCL on blood clearance and hepatic clearance of the test dose of PCL, mice were pretreated with either PSCL (0.625 μmol phospholipids and 12.5 μg siRNA/mouse) or PCL (0.625 μmol phospholipids/mouse). Mice pretreated with 9% sucrose served as the control. At day 5 post-first injection, ^{3}H-CHE labeled PCL (test liposome, 0.625 μmol phospholipids/mouse) was intravenously injected. (a) Blood concentration profile of test liposome. ○, Control; ●, Mice pretreatment with PCL; ▲, Mice pretreatment with PSCL. (b) Hepatic clearance (CLh) of test liposome. Each value represents the mean ± S.D. ($n = 3$ or 4). * $p<0.05$, ** $p<0.01$, *** $p<0.005$.

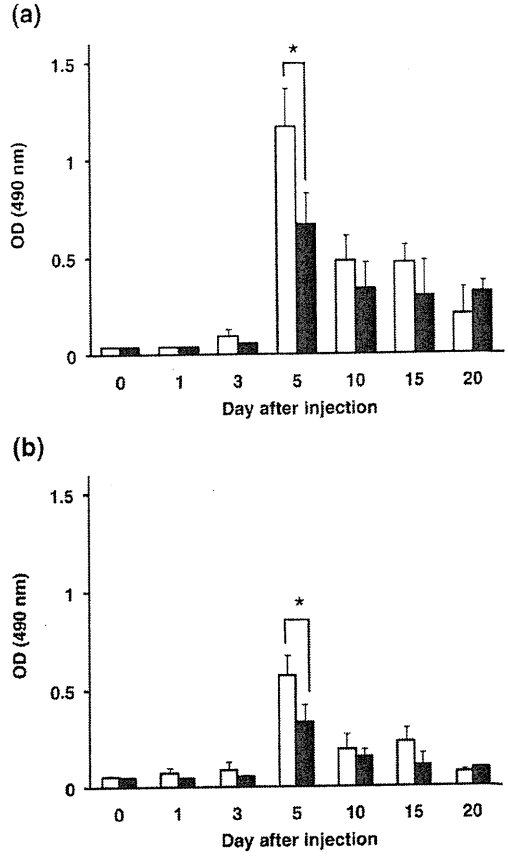

Fig. 3. Time course of changes in anti-PEG IgM and IgG response. Either PSCL (0.625 μmol phospholipids and 12.5 μg siRNA per mouse) or PCL (0.625 μmol phospholipids/mouse) were intravenously injected into the ddY mice. Blood was withdrawn and serum was collected 1–30 days after injection. The sera collected from the naïve mice were used as the control (Day 0). Anti-PEG IgM (a) and IgG (b) were detected using ELISA, as described in the Materials and methods section. □, PCL; ■, PSCL. Each value represents the mean ± S.D. ($n = 4$). * $p<0.05$.

but were persistently detected until day 20, which was the end point of the experiment. Anti-PEG IgM and anti-PEG IgG responses to PSCL were significantly lower than the responses to PCL at day 5 after the injection.

3.3. Anti-PEG IgM response in T cell-deficient (nude) mice

The peak day (day 5) for IgM and IgG responses observed in Fig. 3 was in accordance with a typical T cell-independent (TI) immune response [18]. To confirm whether anti-PEG IgM response to either PSCL or PCL was associated with the TI mechanism, PSCL or PCL was intravenously injected in T cell-deficient (nude) mice. As shown in Fig. 4, an anti-PEG IgM response was detected in both BALB/c nude mice and in BALB/c mice (Fig. 4). In addition, anti-PEG IgM response to PSCL was significantly lower than the response to PCLs in both types of mice ($p<0.05$).

3.4. Effect of splenectomy on anti-PEG IgM production

Our earlier study demonstrated that the spleen plays an important role in anti-PEG IgM production after PEG-coated empty liposome was intravenously administered [10]. Therefore, we investigated the contribution of the spleen to anti-PEG IgM production, induced by the intravenous injection of PSCL or PCL. In splenectomized mice, the anti-PEG IgM response to PSCL or PCL was almost attenuated to the control level (Fig. 5).

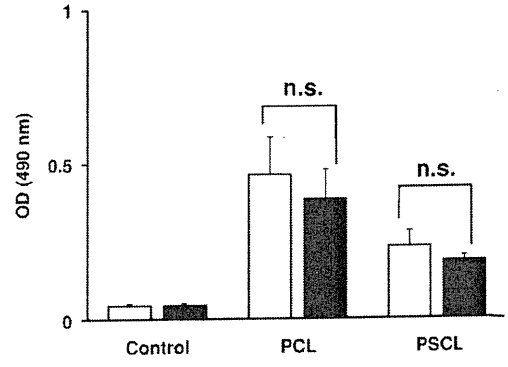

Fig. 4. Anti-PEG IgM responses in T cell-deficient (nude) mice. Either PSCL (0.625 μmol phospholipids and 12.5 μg siRNA/mouse) or PCL (0.625 μmol phospholipids/mouse) were intravenously injected into mice. Five days later, blood was withdrawn and serum was collected. The blood samples collected from the naïve mice were used as controls. Anti-PEG IgM was determined using ELISA, as described in the Materials and methods section. □, BALB/c mice; ■, BALB/c nude mice. Each value represents the mean ± S.D. ($n = 4$). n.s. means not significant.

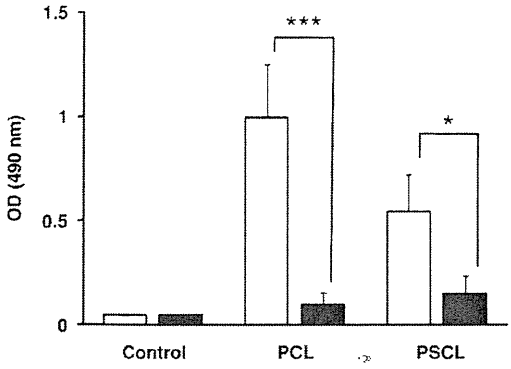

Fig. 5. Effect of splenectomy on anti-PEG IgM response. One day after splenectomy, either PSCL (0.625 μmol phospholipids and 12.5 μg siRNA/mouse) or PCL (0.625 μmol phospholipids/mouse) were intravenously injected into the ddY mice. Five days later, blood was withdrawn and serum was collected. The sera collected from the naïve mice were used as the control. Anti-PEG IgM was detected using ELISA, as described in the Materials and methods section. □, Control; ■, Splenectomy. Each value represents the mean ± S.D. ($n=4$). * $p<0.05$, *** $p<0.005$.

3.5. Splenic clearance of the first dose of PSCL or PCL

The accumulation of either PSCL or PCL in the spleen was determined using either ^{3}H-CHE-labeled PSCL or ^{3}H-CHE-labeled PCL. PSCL showed a slight accumulation (approximately 5% dose/tissue) in the spleen, which was similar to PCL. In addition, splenic clearance (CLs) of PSCL and PCL was calculated (Fig. 6). The CLs of PSCL were higher than those of PCL, suggesting that splenic cells have a greater affinity for PSCL than for PCL, because CLs reflect the affinity of liposomes for the spleen [13].

3.6. The apoptotic effect of PSCL on IgM-expressing B cells in the spleen

The interaction of PSCL or PCL in the spleen, as observed in Fig. 6, might damage IgM-expressing B cells, which produce anti-PEG IgM. On day 5 after the injection, the damage (apoptosis) on IgM-expressing B cells in the spleen was evaluated using a flow cytometer. PSCL significantly induced apoptosis on IgM-expressing B cells (approximately 20% in the IgM-expressing B cells) compared with

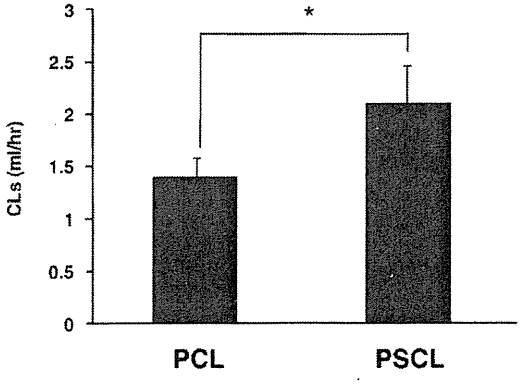

Fig. 6. Splenic clearance after a single intravenous injection of either PSCL or PCL in mice. ^{3}H-CHE labeled PSCL (0.625 μmol phospholipids and 12.5 μg siRNA/mouse) or ^{3}H-CHE labeled PCL (0.625 μmol phospholipids/mouse) were intravenously injected into ddY mice. At selected post-injection time points, blood samples and spleen were collected and radioactivity was measured. The calculation of splenic clearance is described in the Materials and methods section. Each value represents the mean ± S.D. ($n=3$ or 4). * $p<0.05$.

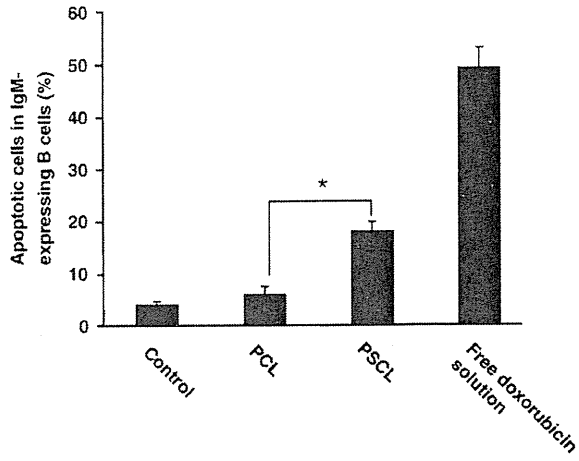

Fig. 7. Apoptotic effect of either PSCL or PCL on IgM-expressing B cells in the spleen. Either PSCL (0.625 μmol phospholipids and 12.5 μg siRNA/mouse) or PCL (0.625 μmol phospholipids/mouse) were intravenously injected into ddY mice. As a positive control, doxorubicin solution (8 mg/kg) was intravenously injected into mice. At 24 h after injection, the splenic cells were collected and treated with "the *in situ* cell death detection kit." IgM-expressing B cells in the splenic cells were gated following staining with anti-mouse IgM antibody. Then the apoptosis of B cells gated were analyzed by flow cytometer. Each value represents the mean ± S.D. ($n=5$). * $p<0.05$.

that of PCL (Fig. 7). On the other hand, PCL showed no apoptotic effect on IgM-expressing B cells.

4. Discussion

The key success factor for siRNA-based therapy has been summarized in the efficacy of the siRNA delivery system [2,3]. The PEG-coated delivery vehicle was endowed with an enormous advantage in the prolonging of blood circulation time for siRNA, but anti-PEG IgM production, would cause the ABC phenomenon, consequently reducing the resident time of siRNA in blood circulation. In this study, we tried to investigate the effect of siRNA in the PEG-coated siRNA-lipoplex (PSCL) on anti-PEG IgM production. Herein, we confirmed that the intravenous injection of both PSCL and PCL induces anti-PEG IgM production (Fig. 1) and consequently causes a second dose of test PCL, injected 5 days later, to lose its long-circulating characteristics and accumulate extensively in the liver (Fig. 2). To the best of our knowledge, this is the first report of anti-PEG IgM production causing the ABC phenomenon by intravenous administration of a PEG-coated vehicle containing siRNA.

In the present study, we found that anti-PEG IgM production was reduced as injected doses were increased (Fig. 1). Such an inverse relationship had already been observed in our previous report using empty PEG-coated neutral liposome in rats [19]. The higher dose might lead the B cells to become inactivated or apoptotic, as described in Fig. 7, and thus inhibit the anti-PEG IgM production. Furthermore, it is noted that the induction of the ABC phenomenon could be prevented by a higher dose of either PSCL or PCL, because the anti-PEG IgM production was completely inhibited by the higher dose (100 μg siRNA and/or 5 μmol, phospholipids/mouse) (Fig. 1). Recent research has shown the successful *in vivo* therapeutic effect of siRNA when preferentially used at a higher dose (100 μg/mouse or more) either with or without PEGylation as a delivery vehicle [2,3]. Such higher doses might be one of the reasons that significant *in vivo* therapeutic effects were achieved with repeated administration. However, minimizing the dosage of siRNA is required for clinical use, since siRNA is still expensive. Hence, ant-PEG IgM production, and the resultant the ABC phenomenon, may emerge as one of essential problems in the use of a PEG-coated vehicle for siRNA delivery.

Splenectomy (removal of the spleen from a mouse) significantly inhibited the production of anti-PEG IgM from pretreatment with

PSCL and PCL (Fig. 5). This suggests that the spleen plays an important role in the immune response to PSCL and PCL. In addition, naïve mice and nude mice, which lack T cells, produced anti-PEG IgM in a similar manner (Fig. 4), suggesting that the immune response against PSCL and PCL in mice is derived in a T cell independent manner. This concern is supported by observations from the time course study on anti-PEG IgM and anti-PEG IgG (Fig. 3). The peak day for anti-PEG IgM and anti-PEG IgG production was in accordance with that of a typical T cell independent immune response [18]. Recently, a similar T cell independent immune response was reported in mice immunized with CpG ODN-containing PEG-coated liposome [20] and ODN-containing PEG-coated liposomes [21].

Our earlier [10,12] and current results strongly indicate that splenic B cells play an important role in the production of anti-PEG IgM in a T cell independent manner. In a general T cell independent immune response, B cells are well known to be activated and produce antibodies by themselves [22,23]. The splenic clearance of PSCL was higher than that of PCL (Fig. 6), although the accumulation amount of PSCL in the spleen was similar to that of PCL (approx. 5% dose/tissue). This suggests that PSCL has a much higher affinity to spleen cells than PCL does, and, therefore, has more chance to interact with splenic B cells. The higher affinity of PSCL than PCL might be due to a difference in surface physicochemical properties of the prepared lipoplexes, between PSCL and PCL. But, due to a lack of basic studies concerning the effect of siRNA on the cationic liposome/lipids in biodistribution, the mechanism of the interaction remains unclear. The greater accessibility of PSCL in comparison with PCL (Fig. 6) might promote more apoptosis in IgM expressing splenic B cells (Fig. 7). Recently, it was reported that siRNA could non-specifically activate cells of the immune system, including the IFN system, and induce the production of cytokines and apoptosis both *in vitro* and *in vivo* [13,24–30]. Moreover, we and other groups have reported *in vitro* studies finding that the expression level of several endogenous genes related to cytokines and apoptosis was enhanced by siRNA transfected by non-viral vectors, Lipofectamine 2000 [31,32] and Oligofectamine [33]. Therefore, we now assume that apoptosis in IgM-expressing B cells could be one of the consequences of non-specific cellular immune responses on IgM-expressing cells and/or splenocytes induced by PSCL, although the precise mechanism remains unclear.

The cell damage by PSCL, observed in Fig. 7, might affect the moderation of anti-PEG IgM production, resulting in different anti-PEG IgM production (Fig. 1) and different ABC phenomenon induction (Fig. 2). Latinne et al. [34] reported that doxorubicin induced apoptosis of B cells and consequently depleted them. We also recently reported that the injection of doxorubicin containing PEG-coated liposome as the first dose dramatically reduced anti-PEG IgM production and consequently diminished the ABC phenomenon [35]. These reports support the theory that the reduction of anti-PEG IgM production may result from apoptosis and inactivation of splenic B cells, although the precise mechanism must be elucidated.

In the early studies, other groups have reported that pDNA and ODN encapsulated in PEG-coated nano-particles greatly enhanced anti-PEG IgM production [13,21]. It is known that nonmethylated bacterial DNA and synthetic ODN can stimulate mononuclear cells and lymphocytes both *in vitro* and *in vivo*, resulting in the secretion of IL6, IL12 and IgM [36]. Hence, the enhancement effect is likely to be attributed to CpG motifs and the palindromic sequence motif. Recent studies indicate that siRNAs, which have specific sequences such as GU-rich, can be potent activators of an innate immune response [24,37,38]. Since siRNA is reportedly recognized by Toll-like receptor-3, -7 and -8 [39], such siRNAs, which have immune stimulatory sequences, may greatly stimulate Toll-like receptors which are expressed in IgM-expressing B cells, and consequently indirectly affect the anti-PEG IgM production induced by the PEG-coated siRNA-lipoplex. The strength of the stimulatory effect on anti-PEG IgM production may be different among siRNA, ODN and pDNA in a sequence-dependent manner. In fact, Li et al. [40] recently reported that PEG-coated lipid nano-particles encapsulated with pDNA significantly induced the secretion of inflammatory cytokines such as IL-6, IL-12 and INF-γ compared to those encapsulated with siRNA.

Nevertheless, the precise mechanism by which PSCL produces anti-PEG IgM and attenuates IgM production remains unknown (Fig. 1). The results of the present study suggest that anti-PEG IgM production is strongly related to the interaction of PSCL with splenic IgM-expressing B cells. Hence, further precise study is required for information that will improve the efficacy of the siRNA delivery system.

5. Conclusion

Our study has significant implications for the use of PEG-coated cationic liposome in the therapeutic evaluation of siRNA drugs. Nonviral, lipid-based delivery systems are generally thought to be nonimmunogenic. PEGylation is expected to attenuate immunogenicity of the carrier components. However, we demonstrated that either PSCL or PCL will activate the immune system, resulting in the production of anti-PEG IgM. Our study presented herein indicates that PEG-coated cationic liposome must be used with caution for applications involving siRNA-based therapeutics, and these results increase the importance of evaluating carrier-directed effects of siRNA-based delivery system.

Acknowledgements

We thank Dr. James L. McDonald for his helpful advice in writing the English manuscript. This work was supported in part by the Health and Labour Sciences Research Grants for Research on Advanced Medical Technology from the Ministry of Health, Labour and Welfare of Japan, and by a Grant-in-Aid for Scientific Research on Priority Areas Cancer, Ministry of Education, Culture, Sports and Technology (20015033).

References

[1] S.M. Elbashir, J. Harborth, W. Lendeckel, A. Yalcin, K. Weber, T. Tuschl, Duplexes of 21-nucleotide RNAs mediate RNA interference in cultured mammalian cells, Nature 411 (2001) 494–498.
[2] S. Akhtar, I.F. Benter, Nonviral delivery of synthetic siRNAs in vivo, J. Clin. Invest. 117 (2007) 3623–3632.
[3] M.A. Behlke, Progress towards in vivo use of siRNAs, Molec. Ther. 13 (2006) 644–670.
[4] P.L. Felgner, T.R. Gadek, M. Holm, R. Roman, H.W. Chan, M. Wenz, J.P. Northrop, G.M. Ringold, M. Danielsen, Lipofection: a highly efficient, lipid-mediated DNA-transfection procedure, Proc. Natl. Acad. Sci. U. S. A. 84 (1987) 7413–7417.
[5] D. Papahadjopoulos, T.M. Allen, A. Gabizon, E. Mayhew, K. Matthay, S.K. Huang, K.D. Lee, M.C. Woodle, D.D. Lasic, C. Redemann, et al., Sterically stabilized liposomes: improvements in pharmacokinetics and antitumor therapeutic efficacy, Proc. Natl. Acad. Sci. U. S. A. 88 (1991) 11460–11464.
[6] V.P. Torchilin, V.G. Omelyanenko, M.I. Papisov, A.A. Bogdanov Jr., V.S. Trubetskoy, J.N. Herron, C.A. Gentry, Poly (ethylene glycol) on the liposome surface: on the mechanism of polymer-coated liposome longevity, Biochim. Biophys. Acta 1195 (1994) 11–20.
[7] Z. Symon, A. Peyser, D. Tzemach, O. Lyass, E. Sucher, E. Shezen, A. Gabizon, Selective delivery of doxorubicin to patients with breast carcinoma metastases by stealth liposomes, Cancer 86 (1999) 72–78.
[8] E.T. Dams, P. Laverman, W.J. Oyen, G. Storm, G.L. Scherphof, J.W. van Der Meer, F.H. Corstens, O.C. Boerman, Accelerated blood clearance and altered biodistribution of repeated injections of sterically stabilized liposomes, J. Pharmacol. Exp. Ther. 292 (2000) 1071–1079.
[9] T. Ishida, H. Kiwada, Accelerated blood clearance (ABC) phenomenon upon repeated injection of PEGylated liposomes, Int. J. Pharm. 354 (2008) 56–62.
[10] T. Ishida, M. Ichihara, X. Wang, H. Kiwada, Spleen plays an important role in the induction of accelerated blood clearance of PEGylated liposomes, J. Control. Release 115 (2006) 243–250.
[11] T. Ishida, M. Ichihara, X. Wang, K. Yamamoto, J. Kimura, E. Majima, H. Kiwada, Injection of PEGylated liposomes in rats elicits PEG-specific IgM, which is responsible for rapid elimination of a second dose of PEGylated liposomes, J. Control. Release 112 (2006) 15–25.
[12] T. Ishida, X. Wang, T. Shimizu, K. Nawata, H. Kiwada, PEGylated liposomes elicit an anti-PEG IgM response in a T cell-independent manner, J. Control. Release 122 (2007) 349–355.
[13] A. Judge, K. McClintock, J.R. Phelps, I. Maclachlan, Hypersensitivity and loss of disease site targeting caused by antibody responses to PEGylated liposomes, Molec. Ther. 13 (2006) 328–337.

[14] Z. Ma, J. Li, F. He, A. Wilson, B. Pitt, S. Li, Cationic lipids enhance siRNA-mediated interferon response in mice, Biochem. Biophys. Res. Commun. 330 (2005) 755–759.
[15] M. Sioud, D.R. Sorensen, Cationic liposome-mediated delivery of siRNAs in adult mice, Biochem. Biophys. Res. Commun. 312 (2003) 1220–1225.
[16] T.M. Allen, P. Sapra, E. Moase, Use of the post-insertion method for the formation of ligand-coupled liposomes, Cell. Mol. Biol. Lett. 7 (2002) 889–894.
[17] H. Harashima, C. Yamane, Y. Kume, H. Kiwada, Kinetic analysis of AUC-dependent saturable clearance of liposomes: mathematical description of AUC dependency, J. Pharmacokinet. Biopharm. 21 (1993) 299–308.
[18] A. Zandvoort, W. Timens, The dual function of the splenic marginal zone: essential for initiation of anti-TI-2 responses but also vital in the general first-line defense against blood-borne antigens, Clin. Exp. Immunol. 130 (2002) 4–11.
[19] T. Ishida, M. Harada, X. Wang, M. Ichihara, K. Irimura, H. Kiwada, Accelerated blood clearance of PEGylated liposomes following preceding liposome injection: effects of lipid dose and PEG surface-density and chain length of the first-dose liposomes, J. Control. Release 105 (2005) 305–317.
[20] W.M. Li, M.B. Bally, M.P. Schutze-Redelmeier, Enhanced immune response to T-independent antigen by using CpG ologodeoxynucleotides encapsulated in liposomes, Vaccine 20 (2001) 148–157.
[21] S.C. Semple, T.O. Harasym, K.A. Clow, S.M. Ansell, S.K. Klimuk, M.J. Hope, Immunogenicity and rapid blood clearance of liposomes containing polyethylene glycol-lipid conjugates and nucleic Acid, J. Pharmacol. Exp. Ther. 312 (2005) 1020–1026.
[22] J.J. Mond, A. Lees, C.M. Snapper, T cell-independent antigens type 2, Annu. Rev. Immunol. 13 (1995) 655–692.
[23] Q. Vos, A. Lees, Z.Q. Wu, C.M. Snapper, J.J. Mond, B-cell activation by T-cell-independent type 2 antigens as an integral part of the humoral immune response to pathogenic microorganisms, Immunol. Rev. 176 (2000) 154–170.
[24] A.D. Judge, V. Sood, J.R. Shaw, D. Fang, K. McClintock, I. MacLachlan, Sequence-dependent stimulation of the mammalian innate immune response by synthetic siRNA, Nat. Biotechnol. 23 (2005) 457–462.
[25] J.T. Marquesand, B.R. Williams, Activation of the mammalian immune system by siRNAs, Nat. Biotechnol. 23 (2005) 1399–1405.
[26] C.A. Sledz, M. Holko, M.J. de Veer, R.H. Silverman, B.R. Williams, Activation of the interferon system by short-interfering RNAs, Nat. Cell Biol. 5 (2003) 834–839.
[27] K. Kariko, P. Bhuyan, J. Capodici, D. Weissman, Small interfering RNAs mediate sequence-independent gene suppression and induce immune activation by signaling through toll-like receptor 3, J. Immunol. 172 (2004) 6545–6549.
[28] S.P. Persengiev, X. Zhu, M.R. Green, Nonspecific, concentration-dependent stimulation and repression of mammalian gene expression by small interfering RNAs (siRNAs), RNA 10 (2004) 12–18.
[29] A. Judge, I. MacLachlan, Overcoming the innate immune response to small interfering RNA, Hum. Gene Ther. 19 (2008) 111–124.
[30] S. Spagnou, A.D. Miller, M. Keller, Lipidic carriers of siRNA: differences in the formulation, cellular uptake, and delivery with plasmid DNA, Biochemistry 43 (2004) 13348–13356.
[31] M.A. Robbins, M. Li, I. Leung, H. Li, D.V. Boyer, Y. Song, M.A. Behlke, J.J. Rossi, Stable expression of shRNAs in human CD34+ progenitor cells can avoid induction of interferon responses to siRNAs in vitro, Nat. Biotechnol. 24 (2006) 566–571.
[32] T. Tagami, K. Hirose, J.M. Barichello, T. Ishida, T.H. Kiwada, Global gene expression profiling in cultured cells is strongly influenced by treatment with siRNA-cationic liposome complexes, Pharm. Res. 25 (2008) 2497–2504.
[33] J.T. Marques, T. Devosse, D. Wang, M. Zamanian-Daryoush, P. Serbinowski, R. Hartmann, T. Fujita, M.A. Behlke, B.R. Williams, A structural basis for discriminating between self and nonself double-stranded RNAs in mammalian cells, Nat. Biotechnol. 24 (2006) 559–565.
[34] D. Latinne, M. Soares, X. Havaux, F. Cormont, B. Lesnikoski, F.H. Bach, H. Bazin, Depletion of IgM xenoreactive natural antibodies by injection of anti-mu monoclonal antibodies, Immunol. Rev. 141 (1994) 95–125.
[35] T. Ishida, K. Atobe, X. Wang, H. Kiwada, Accelerated blood clearance of PEGylated liposomes upon repeated injections: effect of doxorubicin-encapsulation and high-dose first injection, J. Control. Release 115 (2006) 251–258.
[36] A.M. Krieg, CpG motifs in bacterial DNA and their immune effects, Annu. Rev. Immunol. 20 (2002) 709–760.
[37] M. Sioud, Induction of inflammatory cytokines and interferon responses by double-stranded and single-stranded siRNAs is sequence-dependent and requires endosomal localization, J. Mol. Biol. 348 (2005) 1079–1090.
[38] V. Patzel, In silico selection of active siRNA, Drug Discov. Today 12 (2007) 139–148.
[39] M. Sioud, RNA interference and innate immunity, Adv. Drug Deliv. Rev. 59 (2007) 153–163.
[40] S.D. Li, Y.C. Chen, M.J. Hackett, L. Huang, Tumor-targeted delivery of siRNA by self-assembled nanoparticles, Molec. Ther. 16 (2008) 163–169.

Cancer Science
The official journal of the Japanese Cancer Association JCA

Combination therapy of metronomic S-1 dosing with oxaliplatin-containing polyethylene glycol-coated liposome improves antitumor activity in a murine colorectal tumor model

Yusuke Doi, Tomoko Okada, Haruna Matsumoto, Masako Ichihara, Tatsuhiro Ishida[1] and Hiroshi Kiwada

Department of Pharmacokinetics and Biopharmaceutics, Subdivision of Biopharmaceutical Science, Institute of Health Biosciences, The University of Tokushima, Tokushima, Japan

(Received May 23, 2010/Revised July 1, 2010/Accepted July 7, 2010/Accepted manuscript online July 13, 2010/Article first published online August 23, 2010)

Metronomic chemotherapy has been advocated recently as a novel chemotherapeutic regimen. Polyethylene glycol (PEG)-coated liposomes are well known to accumulate in solid tumors by virtue of the highly permeable angiogenic blood vessels characteristic for growing tumor tissue, the so-called "enhanced permeability and retention (EPR) effect". To expand the range of applications and investigate the clinical value of the combination strategy, the therapeutic benefit of metronomic S-1 dosing in combination with oxaliplatin (l-OHP)-containing PEG-coated liposomes was evaluated in a murine colon carcinoma-bearing mice model. S-1 is an oral fluoropyrimidine formulation and metronomic S-1 dosing is a promising alternative to infused 5-FU in colorectal cancer therapy. Therefore, the combination of S-1 with l-OHP may be an alternative to FOLFOX (infusional 5-FU/leucovorin (LV) in combination with l-OHP), which is a first-line therapeutic regimen of a colorectal carcinoma. The combination of oral metronomic S-1 dosing with intravenous administration of liposomal l-OHP formulation exerted excellent antitumor activity without severe overlapping side-effects, compared with either metronomic S-1 dosing, free l-OHP or liposomal l-OHP formulation alone or metronomic S-1 dosing plus free l-OHP. We confirmed that the synergistic antitumor effect is due to prolonged retention of l-OHP in the tumor on account of the PEG-coated liposomes, presumably via alteration of the tumor microenvironment caused by the metronomic S-1 treatment. The combination regimen proposed here may be a breakthrough in treatment of intractable solid tumors and an alternative to FOLFOX in advanced colorectal cancer therapy with acceptable tolerance and preservation of quality of life (QOL). (*Cancer Sci* 2010; 101: 2470–2475)

Oxaliplatin (l-OHP), an innovative third generation platinum compound, has powerful anti-neoplastic competence with no cross drug resistance with cisplatin and carboplatin.[1,2] However, l-OHP shows relatively low anticancer effectivity when it is administered alone, because it shows poor accumulation in tumor tissues due to a high plasma protein binding ratio and high partitioning to erythrocytes, while in addition displaying peripheral neurotoxicity due to high protein binding in the tissue.[3] These features stand in the way of an effective continuous treatment with l-OHP. Oxaliplatin is frequently used for treatment of advanced colorectal cancer when combined with fluorouracil (5-FU) and leucovorin (LV) (FOLFOX).[4,5]

Chemotherapy using nanocarriers as a delivery system has been developed to improve the success of clinical treatment of solid tumors by achieving high accumulation of the chemotherapeutic agent in tumor tissues but with limited accumulation in healthy tissues. Polyethylene glycol (PEG)-modified (PEG-coated) liposomes show prolonged circulating times and thereby enhanced accumulation in solid tumors by virtue of the increased vascular permeability observed in tumor angiogenic blood vessels (the so-called "enhanced permeability and retention (EPR) effect").[6] Therefore, it is reasonable to assume that PEG-coated liposomes may improve the pharmacokinetic features of l-OHP and enhance its anticancer efficiency. We and other groups have shown therapeutic improvement of l-OHP by encapsulation in PEG-coated targeted liposomes.[7–9]

However, nanocarriers of various designs have repeatedly shown insufficient delivery of their payloads to solid tumors. One of the major limitations is insufficiency of the EPR effect due to a disordered intratumoral microenvironment represented for instance by hypovascularity. Recently, Kano *et al.*[10] reported that treatment with transforming growth factor-β type 1 receptor (TβR-1) inhibitor resulted in increased accumulation of nanocarriers accompanied by a pronounced antitumor response in a murine solid tumor model. ten Hagen and co-workers[11,12] have reported a similar observation with tumor necrosis factor α (TNF-α) in both rat and murine models. These approaches are regarded as a breakthrough that can overcome the insufficient EPR effect for nanocarriers in solid tumors. An obvious drawback of this approach is that TβR-1 inhibitor and TNF-α cannot be readily applied because these compounds have not yet been approved for clinical use worldwide.

Metronomic chemotherapy, which refers to the frequent administration of chemotherapeutics at doses significantly below the maximum tolerated dose (MTD) without prolonged drug-free breaks, is a novel approach to the control of advanced cancer.[13,14] The therapy shows a potent anti-angiogenetic effect by targeting genetically stable endothelial cells within the tumor vascular bed, rather than tumor cells with a high mutation rate. Drugs that can be administered orally, such as cyclophosphamide (CPA), capecitabine, UFT and S-1, would meet the requirements of prolonged daily administration schedules. Recently, we showed that metronomic CPA dosing augments intratumoral accumulation of co-administered doxorubicin (DXR)-containing PEG-coated liposomes and this combination exerted an excellent antitumor activity in a murine tumor model without overlapping severe side-effects.[15,16] This favorable therapeutic effect might be attributed to the following mechanism: metronomic dosing with CPA makes the newly forming tumor vessels leaky, and thereby enhances intratumoral accumulation of PEG-coated liposomes.

Oxaliplatin administered together with infusions of 5-FU and LV (FOLFOX) has become a standard treatment regimen for

[1]To whom correspondence should be addressed.
E-mail: ishida@ph.tokushima-u.ac.jp

doi: 10.1111/j.1349-7006.2010.01678.x

advanced colorectal cancer.[4,5] To extend our approach described above, in the present study we evaluated l-OHP/5-FU synergy by combination of metronomic S-1 dosing (orally, daily) with l-OHP-containing PEG-coated liposomes (intravenously, once a week) in a murine colorectal cancer model. S-1 consists of tegaful (a prodrug of 5-FU), 5-chloro-2, 4-dihydroxypyridine (CDHP: an inhibitor of 5-FU degradation) and potassium oxonate (Oxo: a reducer of gastrointestinal toxicity) at a molar ratio of 1:0.4:1. S-1 is one of the most frequently used drugs for oral administration in Japan and shows less toxic side-effects than 5-FU.[17–19] The biochemical modulation of S-1 leads to prolonged retention of 5-FU in the blood, which mimics the pharmacokinetic profile of infusional 5-FU. Daily oral administration with S-1 meets the concept of metronomic dosing and is assumed to enhance intratumoral accumulation of PEG-coated liposomes and l-OHP associated with the liposome.

Materials and Methods

Materials. Hydrogenated soy phosphatidylcholine (HSPC) and 1, 2-distearoyl-sn-glycero-3-phosphoethanolamine-n-(methoxy[polyethylene glycol]-2000) ($mPEG_{2000}$-DSPE) were generously donated by NOF (Tokyo, Japan). Cholesterol (CHOL) was purchased from Wako Pure Chemical (Osaka, Japan). S-1 and l-OHP were generously donated by Taiho Pharmaceutical (Tokyo, Japan). DiI (1, 1′-dioctadecyl-3, 3, 3′,3′-tetramethyl-indocarbocyanine perchlorate) and DiD (1,1′-dioctadecyl-3,3,3′,3′-tetramethyl-indodicarbocyanine perchlorate) were purchased from Invitrogen (Paisley, UK). ^{3}H-Cholesterylhexadecyl ether (^{3}H-CHE) was purchased from Perkin Elmer Japan (Yokohama, Japan). All other reagents were of analytical grade.

Preparation of l-OHP-containing PEG-coated liposomes. l-OHP-containing PEG-coated liposomes, composed of HSPC/CHOL/$mPEG_{2000}$-DSPE (2/1/0.2, molar ratio), were prepared using a reverse-phase evaporation method as described earlier.[9] Unencapsulated, free l-OHP was removed by dialysis by means of a dialysis cassette (Slyde-A-Lyzer, 10000MWCO; Pierce, Rockford, IL, USA) against 5% dextrose. Encapsulated l-OHP was quantified using an atomic absorption photometer (Z-5700; Hitachi, Tokyo, Japan). The phospholipid concentration was determined by colorimetric assay.[20] The particle size of the liposomes was 180 ± 52 nm, as determined with a NICOMP 370 HPL submicron particle analyzer (Particle Sizing System, Mountain View, CA, USA). The encapsulation efficiency of l-OHP was calculated by dividing the drug to lipid ratio after the dialysis by the initial drug to lipid ratio and was approximately 20%. These values are three times higher than that reported recently by another group.

Animal and tumor cell. Male BALB/c mice, 5 weeks old, were purchased from Japan SLC (Shizuoka, Japan). All animal experiments were evaluated and approved by the Animal and Ethics Review Committee of the University of Tokushima.

The Colon 26 (C26) murine colorectal carcinoma cell line was purchased from Cell Resource Center for Biomedical Research (Institute of Development, Aging and Cancer, Tohoku University, Sendai, Japan). To develop tumor-bearing mice, C26 cells (2×10^6) were inoculated subcutaneously into the back of BALB/c mice.

Combination therapy with S-1 and l-OHP formulation. Treatments began when the tumor volumes reached a volume of 40–60 mm^3. The day treatment began was defined as day 0. The dosing schedule of each chemotherapeutic treatment was as follows:

1 Metronomic S-1 dosing: S-1 (6.9 mg tegafur/kg/dose) was administered orally every day from day 0 to day 21.
2 Free or liposomal l-OHP dosing: Free or liposomal l-OHP (4.2 mg/kg/dose) was intravenously administered at day 0, 7 and 14.
3 Combination dosing (S-1 plus free or liposomal l-OHP): S-1 (6.9 mg tegafur/kg per dose) was orally administered daily from day 0 to day 21. Either free or liposomal l-OHP (4.2 mg/kg per dose) was intravenously administered at day 0, 7 and 14.

Tumors were measured externally every third day. Tumor volume was approximated by using formula A below. The antitumor activity was determined by evaluating the change of the relative tumor volume (formula B) and the tumor growth inhibition rate was calculated through formula C.

$$\text{Tumor volume [TV, (mm}^3\text{)]} = 0.5 \times \text{Length} \times \text{Width}^2 \quad \text{(A)}$$

$$\text{Relative tumor volume (RTV)} = \text{Tumor volume on day n/Tumor volume on day 0} \quad \text{(B)}$$

$$\text{Tumor growth inhibtion rate [TGI, (\%)]} = [1 - (\text{mean RTV of treated group})/(\text{mean RTV of control group})] \times 100 \quad \text{(C)}.$$

Effect of S-1 dosing on blood clearance and tumor accumulation of l-OHP encapsulated in PEG-coated liposomes. Treatment with S-1 (6.9 mg tegafur/kg, daily, 7 days) was started when the tumor volumes reached a volume of 40–60 mm^3. To evaluate blood clearance and tumor accumulation of l-OHP encapsulated in PEG-coated liposomes, the liposomal l-OHP formulation (4.2 mg l-OHP/kg) was intravenously injected right after the final S-1 administration. At 6, 12, 24, 36, 48, 72 and 120 h post-injection of l-OHP formulation, plasma was collected, and then the mice were killed to remove the tumor. Tumors were harvested and weighed. Thereafter, concentrated nitric acid was added to the tumor or plasma (100 μL), which was then digested in a microwave oven (600 W for 25 min at 50°C ETHOS TC; Milestone general, Kanagawa, Japan). The content of platinum (Pt) in the plasma and tumor was measured using an ICP-MS (Agilent 7500 series; YOKOKAWA analytical systems, Tokyo, Japan). Europium was added to the assay mixture and calibration standards, respectively. The l-OHP concentrations were calculated from ion counts Pt using the calibration method with internal standard correction. The l-OHP concentration in the tumor was expressed as μg l-OHP per g tissue. Pharmacokinetic parameters were calculated on the basis of l-OHP concentration using poly-exponential curve fitting and the least-squares parameter estimation program SAAM II (SAAM Institute, Seattle, WA, USA).

Effect of S-1 dosing on biodistribution of PEG-coated liposomes. Treatment with S-1 (6.9 mg tegafur/kg, daily, 7 days) was started when the tumor volumes had reached a volume of 40–60 mm^3. To assess the biodistribution of PEG-coated liposomes, ^{3}H-CHE-labeled liposomes (25 mg total lipid/kg) were intravenously injected right after the final S-1 administration. At 24 h after liposome injection, samples (tumor, blood [100 μL], heart, lung, liver, spleen, kidney) were collected. Tissue samples were washed and weighed after removing excess fluid. Radioactivity in the samples was assayed as described previously.[22]

Effect of S-1 dosing on tumor accumulation and distribution of PEG-coated liposomes. Treatment with S-1 (6.9 mg tegafur/kg, daily, 7 days) was started when the tumor volumes had reached a volume of 40–60 mm^3. In order to assess the effect of S-1 dosing on intratumoral accumulation of PEG-coated liposomes, DiI- or DiD-labeled PEG-coated liposomes (25 mg phospholipids/kg) were intravenously injected right after the final S-1 administration. At defined time points (6, 12 and 24 h) after injection, fluorescence imaging was performed with Fluorescence Image Analyzer LAS-4000 IR (Fujifilm, Tokyo, Japan). The fluorescence images were acquired with a 1/100 s exposure

time. For the intratumoral liposome distribution study, at 24 h post-injection, the tumors were harvested and snap-frozen in Optical Cutting Compound (OCT) compound (Sakura Fintechnical, Tokyo, Japan) with dry-iced acetone. Sections of frozen samples (5 μm thick) were directly observed using a fluorescence microscope (Axiovert 200 M; Zeiss, Oberkohen, Germany). Three tumors per group were studied. Thirty images from 10 randomly selected sections per tumor (three images from one section) were analyzed using AxioVision software (Zeiss).

Statistics. All values are expressed as the mean ± SD. Statistical analysis was performed with a two-tailed unpaired *t*-test using GraphPad InStat software (GraphPad Software, La Jola, CA, USA). The level of significance was set at $P < 0.05$.

Results

Tumor growth suppressive effect of metronomic S-1 dosing plus l-OHP-containing PEG-coated liposomes. As shown in Figure 1, free l-OHP showed relatively low antitumor activity compared with other treatments and the TGI was only 19.0%. Metronomic S-1 dosing showed a higher tumor growth suppressive effect than free l-OHP (36.5%, TGI). Liposomal l-OHP showed even a much higher tumor suppressive effect (52.9%, TGI) compared with free l-OHP, and the therapeutic efficiency was very similar to that of conventional combination therapy (metronomic S-1 dosing plus free l-OHP) (57.7%, TGI). Metronomic S-1 dosing plus liposomal l-OHP showed by far the strongest tumor growth suppressive effect (87.0%, TGI) of all treatments. This result indicates that metronomic S-1 dosing combined with l-OHP-containing PEG-coated liposomes produces a superior tumor growth suppressive effect in a murine colorectal tumor model.

To assess toxicity of each mono- or combination therapy, change of bodyweight and blood cells (white cells, red cells and platelets) were determined. Only combination chemotherapy of metronomic S-1 dosing plus l-OHP formulations showed a slight suppression of bodyweight increase. However, there was no significant difference between S-1 plus free l-OHP and S-1 plus liposomal l-OHP (data not shown). In addition there were no significant changes in blood cell counts between each mono- and combination therapy (data not shown).

Effect of metronomic S-1 dosing on clearance and tumor accumulation of l-OHP associated with PEG-coated liposomes. The plasma clearance of l-OHP in S-1 treated mice was very similar to that in control mice; the $t_{1/2}$ in S-1 treated mice amounting to 18.5 h and the $t_{1/2}$ in control mice to 18.1 h. In the tumor without S-1 treatment, l-OHP concentration reached the maximum level (approximately 1500 ng/g tissue) at 24 h after injection, and then precipitously decreased (Fig. 2). In the S-1-treated tumor, l-OHP concentration reached the maximum level, similar to the control, at 24 h after injection, being retained at this level until 48 h and then gradually decreasing (Fig. 2). The area under the concentration–time curve (AUC) of l-OHP in the S-1-treated tumor was approximately 1.4-fold higher than that in the control tumor; 131.6 (μg/g tissue h) in S-1-treated tumor *vs* 96.2 (μg/g tissue h) in the control. These results indicate that the S-1 treatment prolonged the retention of l-OHP within the tumor tissue.

Effect of metronomic S-1 dosing on biodistribution and tumor accumulation of PEG-coated liposomes. To gain more insight into the underlying mechanism of the improved tumor suppressive effect (Fig. 1) and in the prolonged l-OHP retention within the tumor (Fig. 2), we investigated the effect of metronomic S-1 dosing on the biodistribution and tumor accumulation of co-administered PEG-coated liposomes. The effect of daily metronomic S-1 dosing (for 7 days) on the biodistribution of PEG-coated liposomes was investigated with a radio-labeled liposome. The S-1 treatment yielded significant enhancement of accumulation of PEG-coated liposomes (1.3-fold) in tumor at 24 h following administration (Fig. 3). Interestingly, in the S-1-treated mice, there appeared to be a discrepancy between the tumor accumulation of l-OHP (Fig. 2) and liposomes at 24 h following administration. Although the mechanism is uncertain,

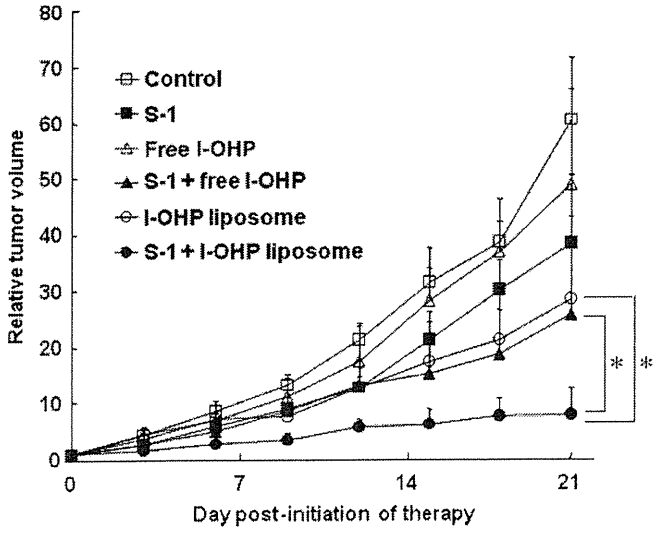

Fig. 1. Antitumor effect of mono- or combination chemotherapy in colorectal tumor-bearing mice. Control (non-treated, □); S-1 dosing (daily, ■); free l-OHP (weekly, △); S-1 dosing (daily) plus free oxaliplatin (l-OHP) (weekly) (▲); l-OHP-containing polyethylene glycol (PEG)-coated liposomes (weekly, ○); S-1 dosing (daily) plus l-OHP-containing PEG-coated liposomes (weekly) (●). Data represent mean ± SD ($n = 5$). *$P < 0.05$.

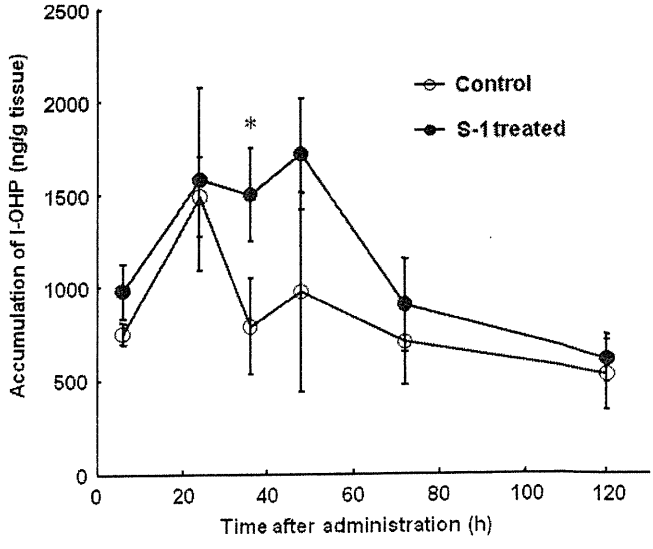

Fig. 2. Effect of S-1 dosing on tumor accumulation of oxaliplatin (l-OHP) delivered by polyethylene glycol (PEG)-coated liposomes. Oxaliplatin-containing PEG-coated liposomes were intravenously administered into tumor-bearing mice that were pre-treated with or without S-1 dosing for 7 days. At various time points, tumor tissue was collected and then l-OHP in the tissue was determined. Data represent mean ± SD ($n = 3$). *$P < 0.05$ *vs* control.

doi: 10.1111/j.1349-7006.2010.01678.x

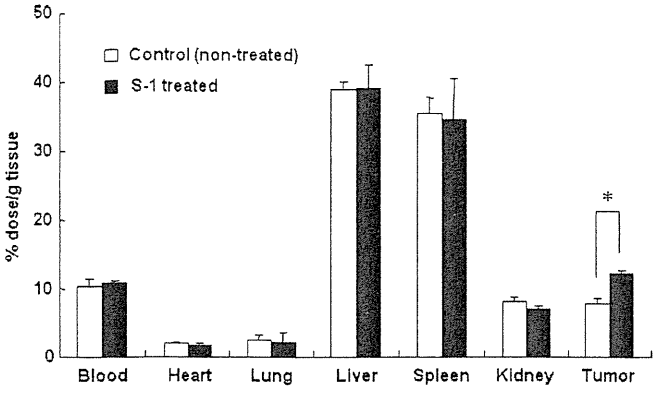

Fig. 3. Effect of S-1 dosing on biodistribution of polyethylene glycol (PEG)-coated liposomes. Biodistribution of PEG-coated liposomes was determined at 24 h following intravenous injection in tumor-bearing mice pretreated with or without S-1 dosing for 7 days. Data represent mean ± SD (n = 3). *P < 0.05.

l-OHP that leaked from the liposome and then bound to plasma proteins and partitioned to erythrocytes might affect the platinum concentration in the tumor. In addition, the treatment did not affect accumulation of PEG-coated liposomes in the major organs (Fig. 3). This observation indicates that the S-1 treatment does not affect the biodistribution of PEG-coated liposomes and the permeability of blood vessels towards the liposomes already existing in normal tissues.

In addition, *in vivo* imaging studies indicated a similar tendency of intratumor accumulation of PEG-coated liposomes as a function of time following injection (Fig. 4). Both the control and S-1-treated mice showed time-dependent augmentation of PEG-coated liposome accumulation. These findings indicate that PEG-coated liposomes accumulated in tumor tissue due to the EPR effect, and S-1 treatment facilitated the EPR effect towards PEG-coated liposomes, resulting in further accumulation of PEG-coated liposomes in solid tumor.

To investigate the intratumoral distribution of PEG-coated liposomes, a histological analysis was carried out. Fluorescence associated with PEG-coated liposomes was observed in the section of both control and S-1-treated tumor (Fig. 5A). The number and size of fluorescence spots in the section of S-1-treated tumor were substantially larger than those in the section of the control tumor, indicating that the S-1 treatment enhanced liposome distribution in tumor tissue. The area density of fluorescence in the tumor section indicated that the sections of S-1 treated tumor contain a much larger amount of PEG-coated liposomes than the section of control tumor (Fig. 5B).

Discussion

In the foregoing section we showed that the combination of oral metronomic S-1 dosing with oxaliplatin (l-OHP)-containing PEG-coated liposomes exerts improved antitumor activity in a murine colorectal tumor model without causing severe side-effects, as compared with conventional combination therapy (metronomic S-1 dosing plus free l-OHP) (Fig. 1). This improvement resulted from enhanced accumulation of l-OHP-containing PEG-coated liposomes and prolonged retention of l-OHP in the tumor induced by metronomic S-1 treatment (Figs 2–5). The FOLFOX regimen (5-FU/LV plus l-OHP) has frequently been used for treatment of advanced colorectal cancer in the clinic.[4,5] However, extended periods of infusional 5-FU (≈48 h) have the disadvantage of increased inconvenience and morbidity of patients related to the use of a portable infusion pump and a central venous catheter. Daily oral administration of

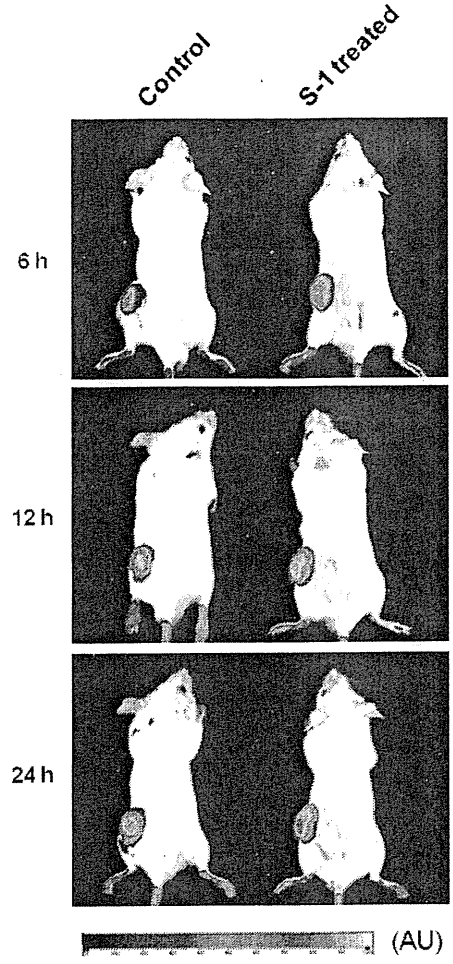

Fig. 4. *In vivo* optical imaging of tumor accumulation of polyethylene glycol (PEG)-coated liposomes. Tumor-bearing mice, pretreated with S-1 dosing for 7 days, received an intravenous injection of DiD (1,1′-dioctadecyl-3,3,3′,3′-tetramethyl-indodicarbocyanine perchlorate)-labeled PEG-coated liposomes. At 6, 12 and 24 h post-injection, *in vivo* optical images were recorded. AU, arbitrary unit.

S-1 can mimic the pharmacokinetic profile of infusional 5-FU and overcome the problems related to infusional 5-FU treatment. In fact, Yamada *et al.*[23] recently reported in a Phase I/II trial that the combination of S-1 with free l-OHP (SOX) is a preferable alternative to the FOLFOX regimen in metastatic colorectal cancer. In contrast to cisplatin, l-OHP has no renal toxicity, only mild hematological and gastrointestinal toxicity, while neurotoxicity is the dose-limiting toxicity.[24,25] The selective delivery of l-OHP to tumors by PEG-coated liposomes raises the possibility of reducing the side-effects of l-OHP in the FOLFOX and SOX regimens. Accordingly, the proposed combination regimen (i.e. addition of S-1 dosing to l-OHP-containing PEG-coated liposomes) may be an alternative to FOLFOX and SOX in advanced colorectal cancer therapy.

Accumulation of nanocarriers into solid tumor after systemic administration is thought to involve the following three processes: (i) distribution through the vascular compartment; (ii) transport across the angiogenic vascular wall (extravasation from neo-vasculature); and (iii) diffusion within the tumor interstitium.[26] It is generally believed that the major target of metronomic chemotherapy is endothelial cells of the growing

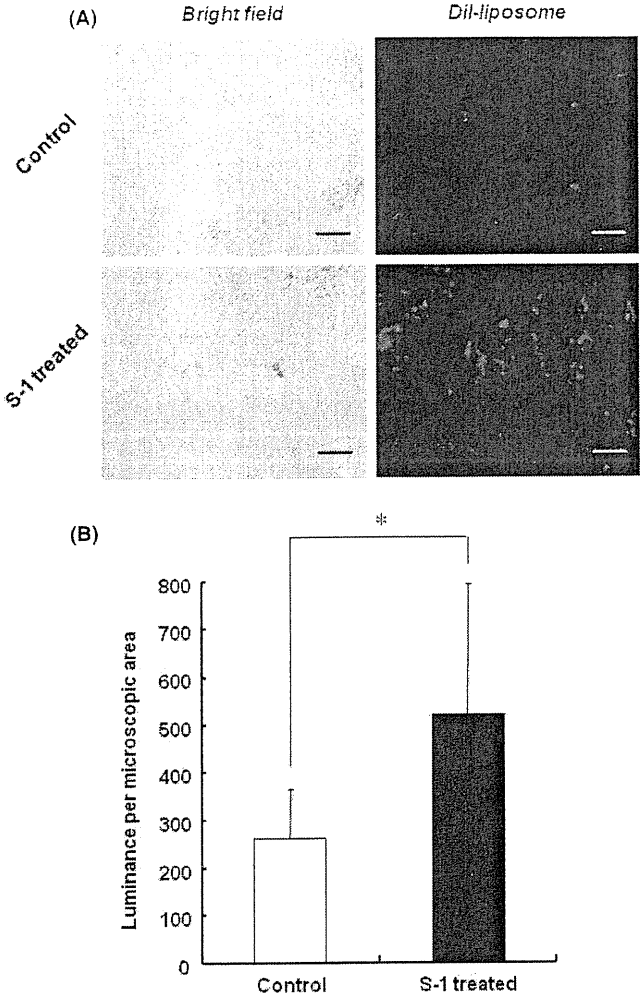

Fig. 5. Effect of S-1 dosing on intratumoral distribution of polyethylene glycol (PEG)-coated liposomes. Tumor-bearing mice, pretreated with S-1 dosing for 7 days, received DiI (1, 1′-dioctadecyl-3, 3, 3′,3′-tetramethyl-indocarbocyanine perchlorate)-labeled PEG-coated liposomes. At 24 h post-injection, the section of tumor was examined with fluorescence microscopy. (A) Intratumoral distribution of PEG-coated liposomes. Red spots represent liposomal distribution. Bar, 100 μm. Original magnification, ×200. (B) Mean fluorescence intensity per microscopic area. Data represent mean ± SD. $*P < 0.05$.

vasculature in the solid tumor. Ooyama *et al.*[27] recently demonstrated that metronomic S-1 dosing damages endothelial cells of tumor vasculature. Loss of the endothelial lining of vessels may make tumor vasculature much leakier. On the basis of our current and previous results,[16] we conclude that the therapy enhances the EPR effect towards PEG-coated liposomes in the following manner: the therapy causes blood vessels in the tumor to become more leaky, resulting in enhanced extravasation of PEG-coated liposomes from the vasculature into the interstitial space of the tumor (Figs 3,4). Moreover, metronomic therapy with S-1 may also exert a cytotoxic effect on viable tumor cells and stromal cells and thus bring about a decrease in the number of both cell types and, consequently, a decrease in the tumor interstitial pressure and enlargement of tumor interstitial space, which, in turn, will allow deeper penetration of the extravasated PEG-coated liposomes (Fig. 5). A similar observation was recently reported by Nagano *et al.*;[28] paclitaxel-induced tumor cell death enhanced the penetration and distribution of virus vector and microspheres in tumor tissue.

In addition to intratumoral accumulation of PEG-coated liposomes, the liposome distribution to major organs was investigated. Metronomic S-1 dosing did not affect accumulation of the liposomes in major organs and blood clearance of the liposomes (Fig. 3). This finding suggests that S-1 treatment does not affect normal vasculature pre-existing in normal tissues, but only the vasculature in tumors, although the mechanism by which S-1 changes only tumor vascular permeability remains unclear. This clearly relates to a safety issue in the proposed combination therapy. In addition, it appears that S-1 treatment does not affect the essential phagocytic uptake activity of hepatic and splenic macrophages, because the treatment did not affect blood clearance of PEG-coated liposomes. Daemen *et al.*[29] have previously reported that injection of DXR-loaded PEG-coated liposomes has a toxic effect on liver macrophages, both in terms of specific phagocytic activity and cell numbers. It is known that defects in the phagocytic uptake mechanism of macrophages can enhance metastatic growth, as reported in numerous animal studies.[30] The cytotoxic effect of l-OHP-containing PEG-coated liposomes on macrophages has not been elucidated yet. Hence, further experiments are in progress to ascertain the alteration of the tumor microenvironment (such as vascular permeability and compressive mechanical force of growing tumor cells) induced by metronomic S-1 dosing and cumulative toxicity of combination therapy of S-1 with l-OHP-containing PEG-coated liposomes.

Anticancer chemotherapy using nanocarriers has shown marked therapeutic effects in many tumor models; however, nanocarriers do not always accumulate effectively in solid tumors, probably due to barriers generated by the tumor microenvironment. Recently, a number of approaches have been introduced that render chemotherapeutics associated with a nanocarrier more efficient. Iyer *et al.*[31] demonstrated that hypertension induced by infusion of angiotensin-II (AT-II) increased the blood flow volume and generated a pressure gradient between the intra- and extravascular space in tumor tissue, resulting in increased extravasation from the tumor vessel of an anticancer agent associated with a nanocarrier. They assumed that the selective accumulation in a solid tumor can be attributed to the absence of a vascular smooth-muscle layer in tumor vasculature. This approach also did not increase the amount of nanocarrier accumulating in healthy organs because of vasoconstriction and tighter endothelial gap junctions of the vasculature. Kano *et al.*[10] demonstrated that low-dose treatment with transforming growth factor-β type 1 receptor inhibitor resulted in further enhanced accumulation of PEG-coated liposomes and micelles to a solid tumor. Seynhaeve *et al.*[12] showed similar results with low-dose TNF-α administration. Our approach also has a potential to achieve enhanced accumulation of PEG-coated liposomes in solid tumors. Hence, the approach that actively causes alteration of the tumor microenvironment by treatment with vaso-active agents or anticancer agents may become a breakthrough in improved delivery of anticancer agents associated with nanocarriers.

Acknowledgments

We thank Dr G.L. Scherphof for his helpful advice on writing the English manuscript. This study was supported in part by a Grant-in-Aid for Young Scientists (A) (21689002), the Ministry of Education, Culture, Sports, Science and Technology, Japan.

Disclosure Statement

No potential conflicts of interest are disclosed.

doi: 10.1111/j.1349-7006.2010.01678.x